A methodological approach to study the stability of selected watercolours for painting reintegration, through reflectance spectrophotometry, Fourier transform infrared spectroscopy and hyperspectral imaging

Claudia Pelosi[1*], Giuseppe Capobianco[2], Giorgia Agresti[1], Giuseppe Bonifazi[2], Fabio Morresi[3], Sara Rossi[1], Ulderico Santamaria[1,3], Silvia Serranti[2]

[1]Department of Economics, Engineering, Society and Business Organization, Laboratory of Diagnostics and Materials Science, University of Tuscia, Largo dell'Università, 01100 Viterbo, Italy
[2]Department of Chemical Engineering Materials & Environment, Sapienza, Rome University, Via Eudossiana 18, 00184 Rome, Italy,
[3]Laboratory of Diagnostics for Conservation and Restoration, Vatican Museums, 001100 Vatican City

***Corresponding author:**
Claudia Pelosi
University of Tuscia
Department of Economics, Engineering, Society and Business Organisation
Laboratory of Diagnostics and Materials Science
Largo dell'Università
01100 Viterbo (Italy)
Tel: +390761357673
Fax: +300761357182
e-mail address: pelosi@unitus.it
Mobile: +393332877468

Abstract

The aim of this work is to investigate the stability to simulated solar radiation of some paintings samples through a new methodological approach adopting non-invasive spectroscopic techniques. In particular, commercial watercolours and iron oxide based pigments were used, these last ones being prepared for the experimental by gum Arabic in order to propose a possible substitute for traditional reintegration materials. Reflectance spectrophotometry in the visible range and Hyperspectral Imaging in the short wave infrared were chosen as non-invasive techniques for evaluation the stability to irradiation of the chosen pigments. These were studied before and after artificial ageing procedure performed in Solar Box chamber under controlled conditions. Data were treated and elaborated in order to evaluate the sensitivity of the chosen techniques in identifying the variations on paint layers, induced by photo-degradation, before they could be observed by eye. Furthermore a supervised classification method for monitoring the painted surface changes adopting a multivariate approach was successfully applied.

Keywords: watercolours stability monitoring, Fourier transform infrared spectroscopy, reflectance spectrophotometry, hyperspectral imaging, multivariate analysis

1. Introduction

The paint layers of art objects are daily subject to aggression by atmospheric agents that, with different mechanisms of degradation, can irreparably damage them. The main causes of alteration in artistic materials are climate, weather and biological agents [**1**]. The relevance of this topic is demonstrated by the first important study on the factors affecting the degradation of artists' materials performed by Russel and de Abney in 1888 and later on further discussed by Brommelle [**2-3**].

The degradation patterns occur also in materials used for conservation, restoration and retouching, sometimes with unknown and unpredictable mechanisms due to the composition of commercial products usually employed by restorers and conservator [**4-7**]. Between these products, watercolours are frequently used for retouching, especially by Italian conservators that, in particular, commonly choose Winsor&Newton as preferred brand **[8]**. Watercolours are produced by the combination of a pigment with gum Arabic and other substances not specified by the manufacturer to safeguard the industrial patent [**9-14**].

Though watercolours are widely used in conservation, their stability in the long run has not been sufficiently studied [**15-21**] or is limited to the investigation of pigment modification without examining the binder behaviour [**22**]. In general, even if retouching is a consolidated praxis in restoration, the monitoring of behaviour of retouched artworks is not widely applied, especially due high costs or lack of maintenance programs. However, several cases of chromatic alteration in areas retouched through watercolours were found, especially in red and brown painting zones where iron based pigments were used [**8**].

In this paper a set of commercial watercolours, normally utilized by conservators, was chosen for stability investigation. In comparison, iron oxide pigments were investigated to verify the possible use of these materials, mixed with gum Arabic, in painting retouching, without any additive. Iron oxide based pigments are stable and widely used for millennia thanks to their stability [**23-24]**. However, when combined with gum Arabic and additives in commercial water colours, the stability of paintings seems to be not the same [**5, 8**]. The choice of apparently quite limited set of samples can be justified by a selection made on the base of a thesis that examined a wide range of water colours and pigment powders [25]. Starting from the results gathered

in the thesis, it was decided to focus the attention on twelve selected painting samples in order to deepen the knowledge of their behaviour to ageing and to test the application of a relatively new analytical approach.

The evaluation of stability of commercial products, used in conservation, can be performed by different analytic and diagnostic techniques, requiring the preparation of a lot of micro-samples to perform the analyses [**26**]. The use of sampling based techniques is not always possible in conservation and monitoring especially due to the difficulty or impossibility to repeat the measurements in the same points and during the time. For this reason, non-invasive no-contact methods were chosen to study and monitoring the photo degradation processes in water colours and pigment powders. In particular, reflectance spectrophotometry in the visible range and HyperSpectral Imaging (HSI) in the short ware infrared region (SWIR) were used with the aim to early detect and monitor the degradation of the investigated painting materials. These techniques were widely applied for the identification and characterization of paint layers but rarely for monitoring of degradation patterns [**27-33**]. In fact, infrared reflectance spectroscopy is well known technique to obtain materials characterization, and to set up correct diagnostic plan based on non-destructive and non-invasive approach [**34-42**]. In particular, SWIR range provides information about vibrational transitions, which are mostly overtones and combination bands whose fundamental transitions occur in the mid-IR. These features are often related to functional groups like hydroxyl (−OH), carbonate ($-CO_3$) and sulphate ($-SO_4$) **[43-44]**. Absorption features from organic materials like the paint binders, can also be observed and used to map their spatial distribution [**30, 45-46**].

HSI, as a diagnostic tool in the field of cultural heritage, is of great interest and presents high potentialities [**47-48**]. If coupled with chemometric techniques, it allows gathering qualitative and/or quantitative information on the nature and physical-chemical characteristics of the investigated materials, and to combine imaging with spectroscopy for evaluating the distribution of materials on the surfaces [**42, 49-53**]. By using classification methods, already applied in other research fields, it is possible to create a predictive model able to identify little variations of the painting layers due to degradation phenomena of the constituent materials [**54-59]**

In conservation of cultural heritage, these classification methods could have great relevance because they allow to monitor in real time the surface changes by observing the spectra variation in respect to the calibration dataset.
For these reasons, in the present work, HSI and visible reflectance spectrophotometry were applied with the following aims: i) to evaluate the sensitivity of the chosen techniques in order to identify the variations on paint layers, induced by photo-degradation, before they could be observed by eye and ii) to use, following a multivariate based approach, the supervised classification methods for the painted surface change monitoring [**52-53**].

2. Materials and Method

2.1 Sample preparation and ageing

As painting materials, some commercial watercolours, professional series supplied by Winsor&Newton both in form of tubes and pans, were selected in order to compare their stability, to light and UV radiation, with that of iron oxide pigments **[60]** supplied by Chroma with the specification of the Country of origin, applied by gum Arabic (GA, by W&N) as binder in order to have the same binder of commercial watercolours. Commercial watercolours were chosen in order to have, for each colour, three typologies: tube, pan and powder. Pan and tube forms were chosen due to their wide use in retouching [**8**]. As selected pigments, yellow ochre, raw umber, raw Sienna and Venetian red were chosen between the most used in retouching **[8]**: in such a way, data from 12 samples will be reported and discussed (Table 1 for sample abbreviations and description). The choice of samples for stability testing was also made on the base of previous data reported in experimental theses [8, 25]. In fact, according to these data, natural umber, yellow ochre, natural Sienna and Venetian red were classified between the less stable water colours, even if they are the most widely used by conservator. For this reason it was chosen to test the possibility of substituting these water colours with materials having the same or similar colour appearance but prepared with natural pigments in powder and gum Arabic, without any additive.

These painting materials were homogeneously applied by brush on traditional gypsum/glue ground (GG) in order to create colour check tables with the different chosen pigments. Gypsum ground was chosen in order to simulate a painting repair to be covered by retouching, as commonly occurs in the practice of restoration of painting lacuna **[8]**. One table was used as blank.

Artificial ageing was performed by using a model 1500E Solar Box chamber (Erichsen Instruments GmbH&Co) that simulates sunlight irradiation (visible and ultraviolet). The system is equipped with a 2.5 kW xenon-arc lamp and UV filter that cuts off the spectrum at 280 nm **[61-62]**. The samples were exposed in the Solar Box chamber from 1 to 504 h at 550 W/m^2, 55°C, and the UV filter at 280 nm. In these conditions, ageing was performed only in relation to light and UV radiation without considering other environmental agents, such as relative humidity. Inside the Solar Box chamber relative humidity was constant (50%) and determined by the irradiation conditions. Relative humidity was monitored by a data logger positioned inside the Solar Box.

2.2 Fourier Transform Infrared (FT-IR) Spectroscopy

A preliminary characterization of pigment samples, before applying them on the ground layer, was performed through Fourier transform infrared spectroscopy (FT-IR). Infrared spectra were obtained using a Nicolet Avatar 360 Fourier transform spectrometer. For each sample 128 scans were recorded in the 4000 to 400 cm^{-1} spectral range (2500-25000 nm) in diffuse reflection modality (DRIFT) with a resolution of 4 cm^{-1}. For FT-IR analysis, 10 mg of each sample was ground in agate mortar with 340 mg of spectrophotometric grade KBr. As background the spectrum of the KBr powder was used. Spectral data were collected with OMNIC 8.0 (Thermo Fisher Scientific Inc.) software.

2.3 Colour monitoring

After exposure for a given length of time the sample table was removed from the Solar Box chamber and the colour was measured using an X-Rite CA22 reflectance spectrophotometer according to the CIELAB1976 colour system, where L* describes the lightness while a* and b* describe the chromatic coordinates on the green-red

and blue-yellow axes, respectively. The characteristics of the colour measuring instrument are the following: colour scale CIEL*a*b*; illuminant D65; standard observer 10°; geometry of measurement 45°/0°; spectral range 400-700 nm; spectral resolution 10 nm; measurement diameter 4 mm. Before taking measurements, the instrument was calibrated with the white reference tile (calibration reference DTP22-62 A013335) supplied by X-Rite, that is a 1x1 cm white ceramic tile.

The differences in lightness (ΔL*), chromatic coordinates (Δa* and Δb*), and total colour (ΔE*) were then calculated using these parameters according to EN 15886 [**63**]. The total colour difference, ΔE*, between two measurements ($L^*_1a^*_1b^*_1$ and $L^*_2a^*_2b^*_2$) is the geometrical distance between their positions in CIELAB colour space. It is calculated using the following equation: $\Delta E^*_{2,1} = [(\Delta L^*)^2 + (\Delta a^*)^2 + (\Delta b^*)^2]^{½}$.

Twelve measures for each colour were performed at the following hour intervals: 0, 168, 336, and 504 hours.

2.4 Hyperspectral imaging (HSI)

Hyperspectral analyses were carried out on sample table at 0, 168, 336 and 504 hours of exposure in the wavelength interval 1000–2500 nm (SWIR). The acquisitions were performed utilizing the SISUChema XL™ (Specim, Finland) device, equipped with a 31 mm lens allowing the acquisition of the paint layer with a resolution of 300 micron/pixel.

The spectral resolution was 6.3 nm. Illumination was obtained by SPECIM's diffuse line illumination unit. Images were acquired through scanning each investigated sample line by line. Instrument is delivered with spectral calibration. Image data is automatically calibrated to reflectance by measuring an internal standard reference target before each sample scan.

The image correction was thus performed adopting the following equation:

$$\boldsymbol{I = \frac{I_0 - B}{W - B} * 100}$$

where $\boldsymbol{I}$ is the corrected hyperspectral image, $\boldsymbol{I_0}$ is the original hyperspectral image, $\boldsymbol{B}$ is the black reference image (~0% reflectance) and $\boldsymbol{W}$ is the white reference image (~99.9% reflectance).

2.5 Spectral analysis

Colour and HSI derived spectral data were analysed by adopting standard chemometric methods [**64-65**], with the PLS_Toolbox (Version 8.2 Eigenvector Research, Inc.) running inside Matlab (Version 8.4, The Mathworks, Inc.). More in details, the spectra preprocessing was performed as follows: raw spectra were preliminary cut, at the beginning and at the end of the investigated wavelength range, in order to eliminate unwanted effects due to lighting/background noise.

Preprocessing was adopted in order to reduce the noise and emphasize the spectral signal [**66-69].** The following preprocessing algorithms were applied: multivariate scatter correction (MSC) to reduce the effect of light scattering; 1^{st} derivative to emphasize the spectral absorption of the investigated paint layers. Finally, Mean Center (MC) was adopted for centering the data before applying principal component analysis.

Principal component analysis (PCA) was applied as a powerful and versatile method capable of providing an overview of complex multivariate data. PCA can be used for revealing relations existing between variables and samples (e.g. clustering), detecting outliers, finding and quantifying patterns, generating new hypotheses as well as many other things [**70**]. In this work, PCA was used to decompose the "processed" spectral data into several principal components (PCs) embedding the spectral variations of each collected spectral data set. The first few PCs, resulting from PCA, are generally utilized to analyze the common features among samples and their grouping: in fact, samples characterized by similar spectral signatures tend to aggregate in the score plot of the first two or three components.

The Soft Independent Modelling of Class Analogy Classification (SIMCA) was then applied as one of the most used class-modeling techniques [**71**]. The SIMCA method is a kind of supervised classification method based on PCA modelling performed for each class in the calibration set. SIMCA is able to use a defined number of PCs for supervised classification. The principal component models for different classes can be updated independently without having to redefine the model [**72-73**]. SIMCA classifications of IR spectra have been reported in the literature in different research areas such as pharmaceutical field [**74**], food research [**75**], medical research [**76**] and environment research [**56**]. Unknown samples are compared to the PCA class

models and assigned to the class according to their analogy with the calibration samples. As this very high within-class variability is covered by the principal components calculated for each class, SIMCA is one of the most commonly used class modelling techniques for the classification of spectral data. After performing a PCA from test data, they have been projected into the n-dimensional data space of each model and assigned to the class with the closest distance. The class assignments were colour coded for display.

3 Results and Discussion

3.1 FT-IR analysis

Fourier transform infrared spectra were displayed in Fig. 1. Powder, tube and pan samples of each selected pigment are reported in the same plot. FT-IR analysis was applied as preliminary screening for highlighting differences and analogies between investigated samples in order to better understand and justify the behaviour of water colours during ageing.

The pan and tube samples clearly show the absorption of gum Arabic in the spectra at (cm^{-1}): 3300-3400 (OH stretching), 2930-2880 (C-H stretching), 1600-1650 (O-H bending), around 1430 (C-H bending), 1040-1070 (C-O stretching) [**77-78**].

Powder yellow ochre (Fig. 1, spectrum 1c) contains calcium carbonate (absorptions at cm^{-1}: 2983, 2874, 2513, 1796, 1445, 877 and 713). This same material is also observed in raw umber powder sample (Fig. 1, spectrum 2c), and in raw Sienna pan and tube samples (Fig. 1, spectra 3a-b). Calcium carbonate is commonly used in commercial pigments and paints as an extender, anti-slip additive, rheology modifier or bulking agents **[79-80]**.

Venetian red powder sample contains high amount of gypsum, as visible in the spectrum 4c (Fig. 1). The typical absorptions of calcium sulphate dihydrate may be observed at cm^{-1}: 3546, 3403, 2237, 2107, 1685, 1621, 1147, 670, 603 and 463. The presence of high amount of gypsum in commercial Venetian red pigments is reported also in the literature [**60, p. 86**].

Characteristic absorption bands of clay minerals (cm^{-1}: 3700-3600, 1100-1000 and 910-800) are observed for yellow ochre (tube and pan, spectra 1a-b in Fig 1), and

raw Sienna powder sample (spectrum 3c in Fig. 1). Apart from being the component of ochre, clay has been widely used as filler and whiting in paints and grounds [**77**, p. 195, **78**].

The preliminary investigation through FT-IR spectroscopy highlighted clear differences between powder samples and commercial pans and tubes watercolours, especially in terms of added materials such as calcium carbonate and gypsum. Some differences can also be observed between tube and pan of the same water colour for yellow ochre (see Fig. 1, spectra 1a and b) in the region 1230-600 cm^{-1} probably due to the presence of different additives in tube and pan.

3.2 Colour data

Colour data were elaborated both in terms of chromatic differences, expressed as ΔL*, Δa*, Δb* and ΔE*, and by PCA in order to observe and discuss the variations induced by light and UV radiation [**81-82**]. We chose to investigate only the effect of radiation on surface layers in order to have the possibility of better testing the chosen methodological approach. Even if other environmental agents are relevant for surface degradation, sunlight, particularly the ultraviolet portion of the solar spectrum is very frequently responsible for the initiation of weathering degradation phenomena [**80, 83-84**]. Environmental conditions can be highly variable, in relation to the exposure conditions of the paintings and to the artificial lighting systems used. The guidelines for exposure in museums and confined environments recommend quite low values of illuminance for organic materials such as water colours. In this case, in fact, 50 lux is suggested as maximum exposure value [85]. But, in real cases, paintings reintegrated with water colours are usually exposed to higher value of illuminance, especially wall paintings that are often located in semi-confined environments or on walls exposed to the outside, as reported in the already mentioned ISCR thesis [8]. For these reasons, there is a manifested necessity for restorers to test water colours and the possibility of using different materials both commercially available and prepared by restorers themselves.

Colour data were obtained and elaborated for each water colour, ground layer and gum Arabic at the various ageing times (Table 2).

By examining the colour differences of gum Arabic and ground, without pigments, it can be derived that some changes occurred as a consequence of ageing, particularly in gum Arabic mainly due to b* decrease and partially to L* increase.
Total color change, expressed by ΔE*, after 504 hours of irradiation is 5.50, a value appreciable by human eye as discussed in the literature [**86**].
Concerning the ground layer, a trend similar to that observed for gum Arabic is found as consequence of irradiation in Solar Box, with the increase of L* (increase of lightness) and decrease of a* and especially b* (decrease of red component), but to a less extent. In fact, the value of ΔE*, after 504 hours of irradiation is 3.00, a change hardly perceptible by human eye [**87**].
However, it should be stressed that the colour coordinates changes for gum Arabic contain also the contribution of the ground layer. In fact, the GA layer is transparent and so colour measurements of this layer are influenced by the ground. So, the changes calculated for GA layer should be considered as a consequence of both gum and gypsum-glue ground.
L* increase and b* decrease can be associated to a probable increase in opacity of the gum Arabic and a loss of the reddish colour that characterizes this binder.
The chromatic changes in the case of pigments are variable in respect to different materials [**86**] but also to different typology (tube, pan or powder) within the same colour, as could be expected if considering the different composition between powders and commercially prepared watercolours and also between pan and tube products.
For example yellow ochre sample in tube exhibits high colour change (ΔE*=6.29 for TY1 after 504 hours of ageing) whereas the same mixture, but commercialized in pan, shows very low variation (ΔE*=1.14 for GY1 after 504 hours of ageing).
In other cases, similar trend in colour changes have been observed for tube and pan samples, such as GBR2 and TBR2 (raw umber), GR2 and TR2 (Venetian red).
Only in one case very high colour changes were calculated, in particular for pan sample GBR4 (raw Sienna). In this case ΔE* value is 21.9 after 504 hours of ageing.
Concerning raw Sienna, high change is also determined for tube sample (ΔE*=8.18 for TBR4 after 504 hours of ageing).

Powder samples applied with gum Arabic as binder exhibit in general low (Y3 and Y10) or negligible (BR10 and R6) changes in colour. This result is quite interesting because it encourages to further test the applicability of natural materials, such as iron oxide pigments, for conservation purposes.

Colour data were also elaborated though PCA and loadings (Figs. 2-6).

To better highlight differences in colour due to ageing, 0 and 504 hours were considered for focusing PCA application.

PCA score plot shows little variations for GG in respect to GA whose changes occur mainly along the first principal component. Loadings describe what principal components represent. In this sense, the loadings vector of PC1 underlines that changes are mainly due to L* (negative) and b* (positive) value.

On the base of this result, it can be hypothesized that gum Arabic is responsible of the grater colour variations in GA layer if compared to GG.

PCA on colour data was applied also for the different water colours selected for testing. Concerning yellow ochre paint samples (Fig. 3), the three tested pigments at time 0 are positioned in different areas of the PCA score plot suggesting different compositions of the mixtures and so expecting different behaviour as consequence of ageing.

By observing the PCA score plot, GY1 appears highly stable to light and UV ageing, in fact it shows no significant variations in the score plot. On the other hand, sample TY1 shows a clear-cut variation along the second PC that, on the base of loadings, is mainly attributable to changes of L* and b* chromatic coordinates.

Powder sample (Y3) has some variations especially along the second principal component that can be associated to L* and b* changes, as visible in the loadings of PCA. As we have hypothesized, the three products exhibit different behaviour in respect to irradiation in Solar Box and this result can be attributed to the different composition.

PCA results on data colour for raw umber samples are reported in Fig. 4.

Sample BR10 is highly stable to light and UV ageing; in fact it undergoes very low variations in the score plot of PCA (Fig. 4A). On the other hand, GBR2 and TBR2 (i.e. commercial watercolours) show a significant variation in colour after ageing.

In particular, the variation of the first component in the PCA score plot is due to all coordinates (Fig. 4B) and it shows the chromatic differences between powder pigments prepared with gum Arabic and commercial watercolours. The variation of second PC is determined mainly by a* (positive) and b* (negative) values and it show the variation related of ageing effects, in particular for watercolour layers. In all samples, binding medium was composed by gum Arabic but the variation in BR10 is almost absent whereas in GBR2 and TBR2 there is a great change along the second component from 0 to 504 hours.

In this case the variations have to be attributed to the pigment and to binder, in combination. Why commercial products vary their colour and pigment powder mixed with gum Arabic shows lower variation? Commercial products are very transparent and do not contain calcium carbonate or other inorganic extenders, in this case the variations of gum Arabic could be relevant. On the other hand, sample BR10 contains calcium carbonate and silicates, and no other organic extenders or additives, so it can be supposed that the influence of binder is not relevant as in tube and pan samples.

The results of PCA applied on data colour for raw Sienna samples are reported in Fig. 5.

In the case of raw Sienna samples, PCA score plot show different positions of pan, tube and powder pigments and also different behaviour to Solar Box ageing. In particular, Y10 sample is highly stable to light and UV ageing; in fact it undergoes very low variations in the score plot of PCA (Fig. 5A, red triangles and empty circles are overlapped). On the other hand, commercial watercolours in pan and tube show high colour changes between 0 and 504 hours of irradiation, especially sample GBR4 that is positioned in two different quadrants of PCA score plot at 0 and 504 hours. Loadings of PCA (Fig. 5B) show that first component variance is due to the three chromatic coordinates whereas the second component variance may be associated to L* (positive) and a* (negative). Water colour sample in pan undergoes a great variation in terms of colour due to irradiation, as also seen previously when discussing ΔE^* values (ΔE^* for GBR4=21.9 at 504 h of ageing). The change of this sample is probably due to the variation of all chromatic coordinates and so it suffers lightness and hue variation clearly appreciable by human eye. It can be hypothesized

that additives in the commercial pan could be responsible of such a great change in colour of raw Sienna sample, combined with gum Arabic variations.
The last examined pigment is Venetian red: the results of PCA are shown in Fig. 6. Also in this case, the three samples are positioned in different area of the scores plot at 0 hours, indicating different compositions of the mixtures.
The scores on PCA show a very low variability in Venetian red samples, in fact they appeared grouped in the plot. Loadings of PCA exhibits that variability along the first component is due to a*, b* (negative) and especially L* (positive), and variability along the second PC is due to a* (negative) and b* (positive) variations. All Venetian red samples appear very stable to ageing, in terms of colour changes and this results suggest the opportunity to use this colour for restoration.

3.3 HSI data

Starting from the acquired raw hypercubes, different regions of interest (ROI) have been selected in order to define, for each studied pigment, a specific area to investigate. Then, at each ageing time, SWIR acquisition was performed and the results have been shown as average and pre-processed spectra. Pre-processing was adopted in order to better highlight the spectral differences between the paintings during ageing times. Spectral area details have been reported to better rate absorption differences between the investigated samples.
With reference to gum Arabic and ground, in Fig. 7 average spectra, spectra detail (2000-2400 nm), and pre-processed spectra are reported.
The average spectra clearly show the contribution of gypsum with the SWIR absorption near 1450, 1490 and 1535 nm, and the OH/H_2O features around 1750 and 1950 nm [**43, 88**] (Fig. 7A). The average spectra of GA exhibit some variation in the region over 2000 nm as a consequence of ageing (Fig. 7B). This behaviour can be attributed to gum Arabic alteration caused by irradiation in Solar Box. On the other hand, ground layer undergoes lower variations. The pre-processed spectra better highlight changes around 2000 and 1200 nm that can be attributed to gum Arabic degradation (Fig. 7C).
The results obtained by PCA show a variance of 99.67% with two principal components and the score plot and loadings are displayed in Fig. 8. The PCA score

plot shows a clear variation along the second principal component between 168 and 336 hours of irradiation for gum Arabic layer (GA1). Ground (GG) shows low variations in the PCA score plot. By examining the loadings of PCA it can be derived that the variance along the second component is mainly due to the absorption around 1400, 1900 and over 2000 nm (Fig. 8B). This result may suggest that the gum Arabic layer decreased in thickness and consequently the absorption of gypsum became more evident in the region of 1400 and 1900 nm. The variance over 2000 nm can be supposed to be due to gum Arabic degradation.

The SIMCA classification model for gum Arabic and setting layer gives the result shown in Fig. 9A-B. The calibration dataset of the model has been set by considering the spectra at time 0. SIMCA model, applied in this modality, allows to see the variation of paint layers for each ageing time in respect to time 0, based on the proximity of unknowns to the different groups in the training set **[88-92]**.

The results outlined in Fig. 9 confirm the representativeness of the selected ROI with a correct identification of painting layers at time 0. Above all, this model allows highlighting the variations of surfaces during time as a consequence of light and UV radiation. In particular, setting layer exhibits no significant variations along time, confirming the relative stability of this layer (Fig. 9B). On the other hand, gum Arabic shows a slow variation and quite homogeneous occurring during ageing time in all part of the sample surface.

The same approach in evaluating the behaviour of the samples with ageing was adopted for paintings with water colours and pigment powders mixed with gum Arabic. In Fig. 10 average spectra, detail of spectra in the range 2000-2350 nm, and pre-processed spectra for yellow ochre samples is displayed.

The analysis of mean spectra shows significant variations between the three pigments and between the ageing times mainly for TY1 and to a less extent for Y3 (Fig. 10A-B).

The differences between the three pigments are visible especially in the region detailed in Fig. 10B (2000-2350 nm) and can be attributed to the presence of different inorganic fractions. In this region, in fact, there are the absorption of calcium carbonate (around 2230, 2341, 2373 nm) and silicates (around 2200 and

2250 nm) **[93]**. $CaCO_3$ is contained in sample Y3 as found by FT-IR spectroscopy (see Fig. 1).

The differences between average spectra due to ageing are better visible in the pre-processed spectra (Fig. 10C). Sample GY1 has no significant variations in spectral features, apart from little changes in the 1400 nm region. On the other hand, TY1 exhibits high variations especially in the region 1200-1400 nm. Sample Y3 undergoes variations in the 1400 nm region but lower than TY1.

The results of PCA on yellow ochre sample are reported in Fig. 11. The captured variance of the model is 90.97% with three principal components. The score plot of PCA reveals immediately a clear-cut compositional difference between the three pigments (at time 0) and also variations, in respect to time 0, of Y3 but especially of TY1. In detail, sample Y3 shows a little change between 0 and 168 h of exposure in Solar Box and a much relevant variation between 168 and 336 hours, with no more significant variation at 504 hours.

Sample TY1 shows significant variation between 0 and 168 hours and also between 168 and 336 hours, confirming the instability to light and UV ageing of this mixture. On the contrary, sample GY1 has low variability with no significant changes in the PCA score plot.

Loadings of PCA for yellow ochre samples highlight two regions with high variance: that between 1000 and 1400 nm where gum Arabic absorptions are located, and that over 2000 nm where the inorganic fraction absorptions are present. The variability in this second region can be attributed to the pigment degradation induced by simulated solar radiation and the consequent reduction of painting layer thickness. As a consequence, the absorptions of calcite and support become more intense.

SIMCA classification model applied to yellow ochre painting samples show that sample GY1 has little variation during time in respect to time 0, concentrated especially on the edges (Fig. 9C). TY1 undergoes a complete change after 168 hours whereas sample Y3 varies lightly after 168 hours of exposure. The variation for Y3 becomes almost complete after 336 hours of irradiation.

The second examined watercolour is raw umber, a brown pigment widely used by conservators for retouching **[8]**. Also in this case, by following the same approach

previously explained, average spectra, detail of spectral region (2050-2500 nm) and pre-processed spectra are reported for raw umber (Fig. 12).

The average spectra show a clear-cut difference between pigment in powder (BR10) and commercial water colours in pan and tube (Fig. 12A). The difference is well-visible especially in the 1000-1500 nm region. The average spectra do not show variation over 2300 nm, related of calcium carbonate and silicates absorptions observable in the 2100-2400 nm region (Fig.12B). The average spectra further highlight the changes occurring during ageing time clearly visible in GBR2 and TBR2 samples. BR10 seems to have less variation in average spectra with irradiation time (Fig. 12A).

In order to better observe the spectral changes over time, pre-processing was applied and the results shown in Fig. 12C confirm the low variations in sample BR10. On the other hand, GBR2 and TBR2 pre-processed spectra allow to highlight strong variations during time especially around 1400 nm (intensity change) and over 1900 nm (wavelength shift).

The model obtained by PCA gives a captured total variance of 96.58%. The scores plot confirms the low variability of sample BR10 and the clear-cut variations of GBR2 and TBR2 (Fig. 13A). In particular, GRB2 and TBR2 show a first variation after 168 h of irradiation occurring along the first PC and a much more significant variation between 168 and 336 h. Loadings of PCA show that time variations, occurring mainly along the first principal component, are correlated to the variations before 1400 nm that can be associated to gum Arabic changes. The variations along the second PC show the variability of organic additives in samples GBR2 and TBR2.

SIMCA model applied to raw umber samples gives the result displayed in Fig. 9D. Also in this case the obtained result confirms the representativeness of selected ROI with a correct identification of painting layers at time 0. But above all this model highlights the variations during ageing times in the painting samples. Sample GBR2 has a clear-cut variation between 168 and 336 hours of irradiation and between 336 and 504 h (clear spectral difference in the pixels between 336 and 504 h). TBR2 changes completely between 168 and 336 h. Sample BR10, on the other hand, has little and slow degradation pattern, mainly concentrated on the edges of the painting layer.

The third examined pigment is raw Sienna and also in this case pan, tube and powder were monitored over ageing time following the same methodological approach used for the other pigments. In Fig. 14 average spectra (A), detail of spectra in the range 2050-2450 nm (B) and pre-processed spectra (C), for raw umber samples.

The analysis of average spectra at time 0 show great differences between powder sample and commercial water colours in pan and tube, visible especially in the region under 1400 nm and over 2100 nm (see Fig. 14B). These differences are mainly due to organic component and also to inorganic fraction. Raw Sienna in powder, in fact, contains kaolinite-like silicates and only traces of calcium carbonate, whereas tube and pan samples contain high amounts of calcium carbonate, as also detected by FT-IR spectroscopy.

The analysis of average spectra, and particularly the pre-processed ones, highlights great variations during ageing times for samples GBR4 and TBR4 especially around 1400 nm. These variations occur both as absorption intensity changes and as shifts in absorption features. The PCA model allows a variance captured of 97.71%. The score plot highlights the changes observed in average spectra for samples GBR4 and TBR4, with a significant variation at all acquired ageing times (Fig. 15A).

In the scores plot of PCA, it can be observed that sample GRB4 varies greatly along the first PC between time 0 and 168 hours and also between 168 and 336 h.

Similar trend is observed for TBR2 even if the variations appear less relevant. On the other hand, sample Y10 shows little variations occurring mainly after 336 h of irradiation. The analysis of loadings (Fig. 15B), in particular that related to PC3, shows that variability derives from absorptions around 1400 nm and over 2000 nm. The variability around 1400 nm is due to the reduction of painting layer and the consequent increase of gypsum absorption, present in the ground layer. The variability over 2000 nm is due to changes in the organic fraction absorptions present in the commercial watercolours.

At last, SIMCA classification was applied to raw Sienna samples and the result is shown in Fig. 9E. Samples GBR4 and TBR4 show a clear difference at time 168 h in respect to time 0, whereas sample Y10 changes after 168 h to become different, in respect to time 0, at 336 hours of irradiation.

The last examined pigment is Venetian red, another pigment selected by conservator for retouching **[8]**. Average spectra are shows in Fig. 16A. They show a clear difference between pigment in powder (R6) and the two commercial water colours in pan and tube (GR2 and TR2). Moreover, the average spectra further show low variability as function of ageing time. The absorption over 2100 nm, that can be associated to the organic additives in water colours are not well visible for Venetian red, probably because they are covered by hydroxyl mineral groups (i.e. Fe-OH at 2230 - 2260 nm).

PCA applied on SWIR data show a captured variance of 95.74 with four principal components and it is confirm the low variability of the three samples with ageing times (Fig. 17A). The score plot highlights three clouds corresponding to the three tested pigments, but the differences related to ageing are very low for each paint layers.

PCA loadings show that the variations along the first component (that identifies the variation due to irradiation) are expressed by the absorptions around 1400 nm and those over 2000 nm (Fig. 17B).

Finally, SIMCA classification applied to spectra taking into account the irradiation time shows that samples start to change after 168 hours of irradiation (Fig. 9F). Sample paintings become completely different after 336 hours. This result suggests that Gum Arabic suffers degradation between 168 and 336 hours whereas the pigments don’t alter at all.

4. Conclusions

Reflectance spectrophotometry in the visible range and Hyperspectral Imaging in the short wave infrared have utilized to evaluate, following a multi-analytical approach, the stability to light and UV ageing of some selected painting materials, in particular powder pigments and commercial watercolours to be used in retouching.

The new methodological approach chosen for monitoring the ageing behaviour of watercolour samples and pigment powder applied by gum Arabic, produced interesting results that should be further discussed and deepened. Different degradation patterns have been observed for the different pigments and also between tube and pan of the same watercolour. Gum Arabic alone clearly shows degradation

occurring between 168 and 336 hours of irradiation. But, when we observe the behaviour of gum Arabic/pigments mixtures, we found that it depends both on the pigment itself but probably also on the combination pigment-gum Arabic and furthermore on the presence of organic additives.

In some cases, the variation of paintings with ageing times is due to gum Arabic, such as in Y3, GBR2, Y10 and in Venetian red samples because it occurs in the same time and with the same pattern observed for gum Arabic alone. On the other hand, sometimes variations are high, such as in samples GBR4, TBR4, TY1, GBR2, TBR2, and can be attribute to both gum Arabic and other components of the mixtures, probable organic additives. In other cases, the combination of gum Arabic and pigment allows to make stable the mixture in regards to light and UV ageing, for example in GY1, BR10, Y3, Y10, GR2, TR2 and R6.

Some authors, through surface investigations, suggested that a thin gum binder layer is present on the surface of watercolour paintings and that other components, such as pigments and additives, are located within the gum layer [**93**]. So, they concluded that the main changes should be attributed to gum Arabic binder. But this result depends on pigment typology, on extender such as calcium carbonate and additives. So, it is quite difficult to predict the behaviour of a specific watercolour.

In general, it can be affirmed that all investigated iron oxide pigments mixed with gum Arabic are stable to ageing under simulated solar radiation and that colour changes are not appreciable by human eye.

Tube samples seem to be the less stable to ageing in Solar Box: apart from Venetian red, in the other cases tube watercolour exhibits high variations as observed in ΔE^* values and also in the SWIR data.

Pan samples have very different behaviour in relation to the pigment: yellow ochre sample (GY1) and Venetian red (GR2) are highly stable to light and UV ageing, whereas raw umber (GBR2) and above all raw Sienna (GBR4) showed low stability to irradiation.

The results point out the potentiality of iron oxide pigments to be used for obtaining stable watercolours, without additives: these ones, in fact, as highlighted in other papers **[5, 8]**, are responsible of variability and degradation in watercolours and they should be better known in order to evaluate the overall stability to ageing of these

commercial materials [**94-95**], especially if they should be used in retouching of artworks, as commonly occurs, especially in the case of wall paintings **[5, 8]**. As final conclusion, it can be affirmed that a correlation of spectrophotometric techniques (i.e. colour data, FT-IR and HSI) coupled with chemometric approach allow to monitor paint layers modifications during ageing time. Furthermore, the classification techniques based on SIMCA, utilizing the hyperspectral data collected by HSI, clearly outlined the potentiality of this approach for monitoring the changes occurring in the painting layers; this was possible thanks to the evaluation of little variations in the spectra during ageing times before that changes can be seen by eyes. We think that this result has great relevance in cultural heritage field because it demonstrated the possibility of detecting damages before they become irreversible. This approach could be particularly useful in monitoring artworks and restoration interventions over times at relatively low cost in respect to other analytical methods.

Acknowledgments

Authors would like to thank Dr. Valeria Valentini, professional restorer, and professor of Restoration of wall paintings at the 5-years Master degree in Conservation and Restoration of Cultural Heritage at University of Tuscia (Viterbo, Italy) for suggestions and help in the choice of watercolours and in their application.

References

[1] D. Camuffo, V. Fassina, J. Havermans, Basic environmental mechanisms affecting cultural heritage. Understanding deterioration mechanisms for conservation purposes, Kermes Quaderni, Nardini Editore, Firenze, 2010.

[2] W. Russell, W. de Abney, Report on the action of light on watercolours to the science and art Department of the Committee of Council on Education, HMSO, London, 1888.

[3] N.S. Brommelle, The Russell and Abney report on the action of light on watercolours, Stud. Conserv. 9 (1964) 140-152, http://dx.doi.org/10.1179/sic.1964.024.

[4] P.M. Whitmore, C. Bailie, Studies on the photochemical stability of synthetic resin-based retouching paints: the effect of white pigments and extenders, Stud. Conserv. 35(1) (1990) 144-149, http://dx.doi.org/10.1179/sic.1990.35.s1.030.
[5] A. Lo Monaco, M. Marabelli, C. Pelosi, R. Picchio, Colour measurements of surfaces to evaluate the restoration materials, in: L. Pezzati, R. Salimbeni (Eds.), Proceedings of SPIE, vol. 8084, SPIE, Digital Library, 2011, pp. 1-14, http://dx.doi.org/10.1117/12.889147.
[6] G. Capobianco, L. Calienno, C. Pelosi, M. Scacchi, G. Bonifazi, G. Agresti, R. Picchio, U. Santamaria, S. Serranti, A. Lo Monaco, Protective behaviour monitoring on wood photo-degradation by spectroscopic techniques coupled with chemometrics, Spectrochim. Acta A 172(5) (2017) 34-42, https://doi.org/10.1016/j.saa.2016.05.050.
[7] S. Digney-Peer, K. Thomas, R. Perry, J. Townsend, S. Gritt, The imitative retouching of easel paintings, in: J.H. Stoner, R. Rushfield (Eds.), Conservation of Easel Paintings (Routledge Series in Conservation and Museology), Routledge, Abingdon-on-Thames (UK), 2012, pp. 607-634.
[8] S. Di Marcello, C. Notarstefano, La verifica della durabilità dei colori ad acquerello impiegati nella reitegrazione pittorica dei dipinti murali, in M. Bonelli, L. D'Agostino, M. Mercalli (Eds.), A Scuola di Restauro, Gangemi Editore, Roma, 2011, pp. 71-81.
[9] M. Größl, S. Harrison, I. Kaml, E. Kenndler, Characterisation of natural polysaccharides (plant gums) used as binding media for artistic and historic works by capillary zone electrophoresis, J. Chromatogr. A 1077 (2005) 80-89, https://doi.org/10.1016/j.chroma.2005.04.075.
[10] B.A. Ormsby, J. H. Townsend, B.W. Singer, J.R. Dean, British watercolour cakes from the eighteenth to the early twentieth century, Stud. Conserv. 50 (2005) 45-66, http://dx.doi.org/10.1179/sic.2005.50.1.45.
[11] S. Caruso, Caratterizzazione e invecchiamento di leganti pittorici a base di gomme vegetali", Thesis, University of Torino, (2006).
[12] I. Bonaduce, H. Brecoulaki, M.P. Colombini, A. Lluveras, V. Restivo, E. Ribechini, Gas chromatographic-mass spectrometric characterisation of plant gums in samples from painted works of art, J. Chromatogr. A 1175 (2007) 275-282, https://doi.org/10.1016/j.chroma.2007.10.056.

[13] V. Kokla, A. Psarrou, V. Konstantinou, Watercolour identification based on machine vision analysis, e-Preservation Science 7 (2010) 22-28.
[14] C. Riedo, D. Scalarone, O. Chiantore, Advances in identification of plant gums in cultural heritage by thermally assisted hydrolysis and methylation, Anal. Bioanal. Chem. 396 (2010) 1159-1569, https://doi.org/10.1007/s00216-009-3325-4.
[15] A. Lerwill, J.H. Townsend, J. Thomas, S. Hackney, C. Caspers, H. Liang, Photochemical colour change for traditional watercolour pigments in low oxygen levels, Stud. Conserv. 60(1) (2015) 15-32, http://dx.doi.org/10.1179/2047058413Y.0000000108.
[16] A. Lewill, Micro-fading spectrometry: an investigation into the display of traditional watercolour pigments in anoxia, PhD Thesis, Nottingham Trent University, 2011.
[17] B. Callede, Stabilité des couleurs utilisées en restauration, pigments bleus", Comité pour la conservation de l'ICOM 4éme Reunion Triennale, Venise, (1975).
[18] E.R. De La Rie, S.Q. Lomax, M. Palmer, L. Deming Glinsman, C.A. Maines, An investigation of the photochemical stability of urea-aldehyde resin retouching paints: removability tests and colour spectroscopy, Stud. Conserv. 45 (Suppl. 1) (2000) 51-59, https://doi.org/10.1179/sic.2000.45.Supplement-1.51.
[19] G. Korenberg, The photo-ageing behaviour of selected watercolour paints under anoxic conditions, The British Museum Technical Research Bulletin 2 (2008) 49-57.
[20] E. Kampasakali, A.P. Moutsatsou, D. Christofilos, E.A.Varella, Preliminary study on the effects of accelerated ageing on the chromatic profile of gouache and watercolour paint layers on paper, in: 8th International Conference on Non-destructive investigations and microanalysis for the diagnostics and conservation of the cultural and environmental heritage, Lecce (Italy), 15-19 May 2005.
[21] P. Dellaportas, E. Papageorgiou, G. Panagiaris, Museum factors affecting the ageing process of organic materials: review on experimental designs and the INVENVORG project as a pilot study, Herit. Sci. 2(2) (2014) 1-11, https://doi.org/10.1186/2050-7445-2-2.
[22] A. Bailão, M. San Andrés, A. Calvo, Colorimetric analysis of two watercolours used in retouching, International Journal of Conservation Science 5(3) (2014) 329-342.

[23] J. Clarke, Two aboriginal rock art pigments from western Australia: their properties, use, and durability, Stud. Conserv. 21(3) (1976) 134-142, doi: 10.2307/1505696.
[24] H.W. Levison, Artists' pigments: lightfastness tests and ratings: the permanency of artists' colors and an evaluation of modern pigments, Hallandale, Fla., 1976, 85 p.
[25] S. Rossi, Studio della stabilità di acquerelli commerciali e pigmenti naturali per la reintegrazione dei beni culturali, Thesis, University of Tuscia, 2016.
[26] P. Ropret, R. Zoubek, A. Sever Škapin, P. Bukovec, Effects of ageing on different binders for retouching and on some binder–pigment combinations used for restoration of wall paintings, Mater. Charact. 58(11) (2007) 1148-1159, http://dx.doi.org/10.1016/j.matchar.2007.04.027.
[27] C. Pelosi, M. Marabelli, F. Patrizi, F. Ortenzi, F. Giurlanda, C. Falcucci, Valutazione della stabilità degli acquerelli nel restauro attraverso misure di colore, Atti della V Conferenza Nazionale del Gruppo Colore, StarryLink Editrice, Brescia, 141-149 (2009).
[28] M. Kubik, Hyperspectral imaging: a new technique for the non-invasive study of artworks, Physical Techniques in the Study of Art, Archaeology and Cultural Heritage, 2 (2007) 199-259, https://doi.org/10.1016/S1871-1731(07)80007-8.
[29] M. Aceto, A. Agostino, G. Fenoglio, A. Idone, M. Gulmini, M. Picollo, P. Ricciardi, J.K. Delaney, Characterisation of colourants on illuminated manuscripts by portable fibre optic UV-visible-NIR reflectance spectrophotometry, Anal. Methods 6 (2014) 1488-1500, doi:10.1039/c3ay41904e.
[30] J.K. Delaney, J.G. Zeibel, M. Thoury, R. Littleton, M. Palmer, K.M. Morales, E.R. De la Rie, A. Hoenigswald, Visible and infrared imaging spectroscopy of Picasso's Harlequin musician: mapping and identification of artist materials in situ, Appl. Spectrosc. 64(6) (2010) 584-594, https://doi.org/10.1366/000370210791414443.
[31] F. Rosi, C. Grazia, F. Gabrieli, A. Romani, M. Paolantoni, R. Vivani, B.G. Brunetti, P. Colomban, C. Miliani, UV–Vis-NIR and micro Raman spectroscopies for the non destructive identification of $Cd_{1-x}Zn_xS$ solid solutions in cadmium yellow pigments, Microchem. J. 124 (2016) 856–867, https://doi.org/10.1016/j.microc.2015.07.025.

[32] C. Miliani, F. Rosi, B.G. Brunetti, A. Sgamellotti, In situ noninvasive study of artworks: the MOLAB multitechnique approach, Acc. Chem. Res. 43(6) (2010) 728–738, doi:10.1021/ar100010t.
[33] C. Balas, V. Papadakis, N. Papadakis, A. Papadakis, E. Vazgiouraki, G. Themelis, A novel hyper-spectral imaging apparatus for the non-destructive analysis of objects of artistic and historic value, J. Cult. Herit. 4(1) (2003) 330-337, https://doi.org/10.1016/S1296-2074(02)01216-5.
[34] R.D. Rusu, B. Simionescu, A.V. Oancea, M. Geba, L. Stratulat, D. Salajan, L.E. Ursu, M.C. Popescu, M. Dobromir, M. Murariu, C. Cotofana, M. Olaru, Analysis and structural characterization of pigments and materials used in Nicolae Grigorescu heritage paintings, Spectrochim. Acta A 168 (2016) 218-229, https://doi.org/10.1016/j.saa.2016.06.009.
[35] I. Arrizabalaga, O. Gómez-Laserna, J. Aramendia, G. Arana, J.M. Madariaga. Applicability of a diffuse reflectance infrared Fourier transform handheld spectrometer to perform in situ analyses on cultural heritage materials, Spectrochim. Acta A 129 (2014) 259-267, https://doi.org/10.1016/j.saa.2014.03.096.
[36] I. Arrizabalaga, O. Gómez-Laserna, J. Aramendia, G. Arana, J.M. Madariaga, Determination of the pigments present in a wallpaper of the middle nineteenth century: the combination of mid-diffuse reflectance and far infrared spectroscopies, Spectrochim. Acta A 124 (2014) 308-314, https://doi.org/10.1016/j.saa.2014.01.017.
[37] E.L. Von Aderkas, M.M. Barsan, D.F. Gilson, I.S. Butler, Application of photoacoustic infrared spectroscopy in the forensic analysis of artists' inorganic pigments, Spectrochim. Acta A 77(5) (2010) 954-959, https://doi.org/10.1016/j.saa.2010.08.027.
[38] M.A. Maynez-Rojas, E. Casanova-González, J.L. Ruvalcaba-Sil, Identification of natural red and purple dyes on textiles by fiber-optics reflectance spectroscopy. Spectrochim. Acta A, 178 (2017) 239-250, https://doi.org/10.1016/j.saa.2017.02.019.
[39] B. Trzcińska, R. Kowalski, J. Zięba-Palus, Comparison of pigment content of paint samples using spectrometric methods, Spectrochim. Acta A 130 (2014) 534-538, https://doi.org/10.1016/j.saa.2014.03.099.

[40] L. Rampazzi, V. Brunello, C. Corti, E. Lissoni, Non-invasive techniques for revealing the palette of the Romantic painter Francesco Hayez, Spectrochim. Acta A 176 (2017) 142-154, https://doi.org/10.1016/j.saa.2017.01.011.
[41] S. Carlesi, G. Bartolozzi, C. Cucci, V. Marchiafava, M. Picollo, J. La Nasa, F. Di Girolamo, M. Dilillo, F. Modugno, I. Degano, M.P. Colombini, S. Legnaioli, G. Lorenzetti, V. Palleschi, Discovering "The Italian Flag" by Fernando Melani (1907–1985), Spectrochim. Acta A 168 (2016) 52-59, https://doi.org/10.1016/j.saa.2016.05.027.
[42] G. Capobianco, G. Bonifazi, F. Prestileo, S. Serranti, Pigment identification in pictorial layers by Hyper-spectral Imaging, Proceedings of SPIE, Volume 9106, Article number 91060B, 2014, http://dx.doi.org/10.1117/12.2049941.
[43] J.K. Delaney, M. Thoury, J.G. Zeibel, P. Ricciardi, K.M. Morales, K.A. Dooley, Visible and infrared imaging spectroscopy of paintings and improved reflectography, Heritage Science 4(6) (2016) 1-10, https://doi.org/10.1186/s40494-016-0075-4.
[44] R.N. Clark, Spectroscopy of rocks and minerals, and principles of spectroscopy, in: A.N. Rencz (ed.), Manual of remote sensing, remote sensing for the earth sciences, vol. 3, Wiley, New York, 1999, pp. 3–58.
[45] P. Ricciardi, J.K Delaney, M. Facini, J.G. Zeibel, M. Picollo, S. Lomax, M. Loew, Near infrared reflectance imaging spectroscopy to map paint binders in situ on illuminated manuscripts, Angew. Chem. Int. Edit. 51 (2012) 5607–5610, doi: 10.1002/anie.201200840.
[46] K.A. Dooley, S. Lomax, J.G. Zeibel, C. Miliani, P. Ricciardi, A. Hoenigswald, M. Loew, J.K. Delaney, Mapping of egg yolk and animal skin glue paint binders in Early Renaissance paintings using near infrared reflectance imaging spectroscopy, Analyst 138 (2013) 4838–4848, DOI: 10.1039/c3an00926b.
[47] A. Polak, T. Kelman, P. Murray, S. Marshall, D.J.M. Stothard, N. Eastaugh, F. Eastaugh, Hyperspectral imaging combined with data classification techniques as an aid for artwork authentication, J. Cult. Herit. 26 (2017) 1-11, http://dx.doi.org/10.1016/j.culher.2017.01.013.
[48] M. Zucco, M. Pisani, T. Cavaleri, Fourier transform hyperspectral imaging for cultural heritage, in: Fourier transforms - high-tech application and current trends, INTECH, (2017), pp. 215-234 , http://dx.doi.org/10.5772/66107.

[49] G. Capobianco, M.P. Bracciale, D. Sali, F. Sbardella, P. Belloni, G. Bonifazi, S. Serranti, M.L. Santarelli, M. Cestelli Guidi, Chemometrics approach to FT-IR hyperspectral imaging analysis of degradation products in artwork cross-section, Microchem. J. 132 (2017) 69-76, https://doi.org/10.1016/j.microc.2017.01.007.
[50] C. Fischer, I. Kakoulli, Multispectral and hyperspectral imaging technologies in conservation: current research and potential applications, Stud. Conserv. 51(Suppl. 1) (2006) 3–16, http://dx.doi.org/10.1179/sic.2006.51.Supplement-1.3.
[51] E. Catelli, L.L. Randeberg, B.K. Alsberg, K.F. Gebremariam, S. Bracci, An explorative chemometric approach applied to hyperspectral images for the study of illuminated manuscripts, Spectrochim. Acta A 177 (2017) 69-78, https://doi.org/10.1016/j.saa.2017.01.015.
[52] G. Agresti, G. Bonifazi, L. Calienno, G. Capobianco, A. Lo Monaco, C. Pelosi, R. Picchio, S. Serranti, Surface investigation of photo-degraded wood by colour monitoring, infrared spectroscopy and hyperspectral imaging, J. Spectrosc. 1 (1) (2013) article ID 380536, http://dx.doi.org/10.1155/2013/380536.
[53] G. Bonifazi, L. Calienno, G. Capobianco, A. Lo Monaco, C. Pelosi, R. Picchio, S. Serranti, Modelling color and chemical changes on normal and red heart beech wood by reflectance spectrophotometry, Fourier Transform infrared spectroscopy and hyperspectral imaging, Polym. Degrad. Stabil. 113 (2015) 10-21, https://doi.org/10.1016/j.polymdegradstab.2015.01.001.
[54] F. Westad, F. Marini, Validation of chemometric models - A tutorial, Anal. Chim. Acta 893 (2015) 14–24, doi:10.1016/j.aca.2015.06.056.
[55] M.Á. de la Ossa, C. García-Ruiz, J.M. Amigo, Near infrared spectral imaging for the analysis of dynamite residues on human handprints, Talanta, 130 (2014) 315–321, doi: 10.1016/j.talanta.2014.07.026.
[56] G. Bonifazi, G. Capobianco. S. Serranti, Asbestos containing materials detection and classification by the use of hyperspectral imaging, J. Hazard. Mater. 344 (2017) 981–993, doi: 10.1016/j.jhazmat.2017.11.056.
[57] J. Burger, P. Geladi, Hyperspectral NIR image regression part II: Dataset preprocessing diagnostics, J. Chemometr. 20 (2006) 106–119, doi:10.1002/cem.986.
[58] S.M. van Ruth, B. Villegas, W. Akkermans, M. Rozijn, H. van der Kamp, A. Koot, Prediction of the identity of fats and oils by their fatty acid, triacylglycerol and

volatile compositions using PLS-DA, Food Chem. 118(4) (2010) 948–955, doi:10.1016/j.foodchem.2008.10.047.
[59] K.N. Basri, M.N. Hussain, J. Bakar, Z. Sharif, M.F.A. Khir, A.S. Zoolfakar, Classification and quantification of palm oil adulteration via portable NIR spectroscopy, Spectrochim. Acta A 173 (2017) 335-342, https://doi.org/10.1016/j.saa.2016.09.028.
[60] K. Helwig, Iron oxide pigments, in: B.H. Barrie (Ed.), Artistis' pigments. A handbook of their history and characteristics, National Gallery of Art, Washington and Archetype Publications, London, 2007, pp. 39-109.
[61] ISO 16474-1, Paint and Varnishes: Methods of exposures to laboratory light sources-Part 1: General guidance, Geneva (Switzerland) 2013.
[62] ISO16474-2, Paint and Varnishes-Methods of exposure to laboratory light sources-Part 1: Xenon-arc lamp, Geneva (Switzerland) 2013.
[63] EN 15886, Conservation of cultural property-Test Methods — Colour measurement of surfaces, Brussels (Belgium), 2010.
[64] H. Grahn, P. Geladi, J. Burger, in: H. Grahn, P. Geladi (Eds.), Techniques and applications of hyperspectral image analysis, John Wiley & Sons, West Sussex, 2007, pp. 1–15.
[65] M. Otto, Chemometrics, statistics and computer application in analytical chemistry, Wiley-VCH, New York, 1999.
[66] M. Vidal, J.M. Amigo, Pre-processing of hyperspectral images. Essential steps before image analysis, Chemometr. Intell. Lab. 117 (2012) 138-148, https://doi.org/10.1016/j.chemolab.2012.05.009.
[67] Å. Rinnan, F. van den Berg, S.B. Engelsen. Review of the most common pre-processing techniques for near-infrared spectra, TrAC-Trend Anal. Chem. 28(10) (2009) 1201-1222, https://doi.org/10.1016/j.trac.2009.07.007.
[68] J.M. Amigo, H. Babamoradi, S. Elcoroaristizabal, Hyperspectral image analysis. A tutorial, Anal. Chim. Acta 896 (2015) 34-51, https://doi.org/10.1016/j.aca.2015.09.030.
[69] Å. Rinnan, L. Nørgaard, F. van den Berg, J. Thygesen, R. Bro, S.B. Engelsen, Data pre-processing, in: D.-W. Sun (Ed.) Infrared spectroscopy for food quality

analysis and control, Chapter 2, 2009, pp. 29-50, https://doi.org/10.1016/B978-0-12-374136-3.00002-X.
[70] R. Bro, A. K. Smilde, Principal component analysis, Anal. Methods 6 (2014) 2812-2831, DOI: 10.1039/C3AY41907J.
[71] R. De Maesschalck, A. Candolfi, D.L. Massart, S. Heuerding, Decision criteria for soft independent modelling of class analogy applied to near infrared data, Chemometr. Intell. Lab. 47(1) (1999) 65-77, https://doi.org/10.1016/S0169-7439(98)00159-2.
[72] Y. Roggo, L. Duponchel, J.P. Huvenne, Comparison of supervised pattern recognition methods with McNemar's statistical test: application to qualitative analysis of sugar beet by near-infrared spectroscopy, Anal. Chim. Acta 477(2) (2003) 187-200, https://doi.org/10.1016/S0003-2670(02)01422-8.
[73] O. Galtier, O. Abbas, Y. Le Dréau, C. Rebufa, J. Kister, J. Artaud, N. Dupuy, Comparison of PLS1-DA, PLS2-DA and SIMCA for classification by origin of crude petroleum oils by MIR and virgin olive oils by NIR for different spectral regions, Vib. Spectrosc. 55(1) (2011) 132-140, https://doi.org/10.1016/j.vibspec.2010.09.012.
[74] M. Foot, M. Mulholland, Classification of chondroitin sulfate A, chondroitin sulfate C, glucosamine hydrochloride and glucosamine 6 sulfate using chemometric techniques, J. Pharm. Biomed. Anal. 38(3) (2005) 397-407, https://doi.org/10.1016/j.jpba.2005.01.026.
[75] R. Bauer, H. Nieuwoudt, F.F. Bauer, J. Kossmann, K.R. Koch, K.H. Esbensen, FTIR spectroscopy for grape and wine analysis, Anal. Chem. 80(5) (2008), 1371-1379, DOI: 10.1021/ac086051c.
[76] C. Krafft, L. Shapoval, S.B. Sobottka, G. Schackert, R. Salzer, Identification of primary tumors of brain metastases by infrared spectroscopic imaging and linear discriminant analysis, Technol. Cancer Res. Treat. 5(3) (2006) 291-298, https://doi.org/10.1177/153303460600500311.
[77] M.R. Derrick, D. Stulik, J.M. Landry, Infrared spectroscopy in conservation science, The Getty Conservation Institute, Los Angeles, 1999.
[78] W. Vetter, M. Schreiner, Characterization of pigment-binding media systems – Comparison of non-invasive in-situ reflection FTIR with transmission, e-Preservation Science 8 (2011) 10-22.

[79] N. Sano, P.J. Cumpson, Surface analysis characterisation of gum binders used in modern watercolour paints, Appl. Surf. Sci. 364 (2016) 870-877, https://doi.org/10.1016/j.apsusc.2015.12.162.
[80] R.J. Gettens, E.W. FitzHugh, R.L. Feller, Calcium carbonate whites, in: A. Roy (Ed.), Artists' pigments. A handbook of their history and characteristics, National Gallery of Art, Washington, 1993, pp. 203-226.
[81] R.L. Feller, Accelerated aging. Photochemical and thermal aspects, The Getty Conservation Institute, Los Angeles, 1994.
[82] S. Michalski, Damage to museum objects by visible radiation (light) and ultraviolet radiation (UV). Lighting in museums galleries and historical houses, Bristol seminar, Museums Association, London, 1987, pp. 3-16.
[83] R.P. Brown, Survey of status of test methods for accelerated durability testing, Polym. Test. 10(1) (1991) 3-30, https://doi.org/10.1016/0142-9418(91)90038-Y.
[84] D. Kockott, Natural and artificial weathering of polymers, Polym. Degrad. Stab. 25(2-4) (1989) 181-208, https://doi.org/10.1016/S0141-3910(89)81007-9.
[85] UNI 10829, Beni di interesse storico e artistico - Condizioni ambientali di conservazione - Misurazione ed analisi, Milano, 1999.
[86] W. Mokrzycki, M. Total, Color difference Delta E - A survey, Machine Graphics and Vision 20(4) (2011) 383-411.
[87] C. Pelosi, M. Marabelli, F. Patrizi, F. Ortenzi, F. Giurlanda, C. Falcucci, Valutazione degli acquerelli nel restauro attraverso misure di colore, in F. Prestileo, A. Rizzi (Eds.), Colore e Colorimetria: Contributi Multidisciplinari Vol. V, Starrylink, 2009, pp. 141-149.
[88] F. Velasco, A. Alvaro, S. Suarez, J.-M. Herrero, I. Yusta, Mapping Fe-bearing hydrated sulphate minerals with short wave infrared (SWIR) spectral analysis at San Miguel mine environment, Iberian Pyrite Belt (SW Spain), J. Geochem. Explor. 87 (2005) 45–72, https://doi.org/10.1016/j.gexplo.2005.07.002.
[89] W. Fremout, S. Kuckova, M. Crhova, J. Sanyova, S. Saverwyns, R. Hynek, M. Kodicek, P. Vandenabeele, L. Moens, Classification of protein binders in artist's paints by matrix-assisted laser desorption/ionisation time-of-flight mass spectrometry: and evaluation of principal component analysis (PCA) and soft

independent modelling of class analogy (SIMCA), Rapid Commun. Mass Spectrom. 25 (2011) 1631-1640, doi: 10.1002/rcm.5027.
[90] S. Duchêne, V. Detalle, R. Bruder, J.B. Sirven, Chemometrics and Laser Induced Breakdown Spectroscopy (LIBS) analyses for identification of wall paintings pigments, Curr. Anal. Chem. 6(1) (2010) 60-65, DOI: 10.2174/157341110790069600.
[91] R. Checa-Moreno, E. Manzano, G. Mirón, L.F. Capitan-Vallvey, Comparison between traditional strategies and classification technique (SIMCA) in the identification of old proteinaceous binders, Talanta 75 (2008) 697-704, https://doi.org/10.1016/j.talanta.2007.12.020.
[92] M. Hoehse, A. Paul, I. Gornushkin, U. Panne, Multivariate classification of pigments and inks using combined Raman spectroscopy and LIBS, Anal. Bioanal. Chem. 402 (2012) 1443-1450, https://doi.org/10.1007/s00216-011-5287-6.
[93] R.N. Clark, T.V.V King, M. Klejwa, G.A. Swayze, N. Vergo, High spectral resolution reflectance spectroscopy of minerals. J. Geophys. Res. 95 (1990) 12653–12680, DOI: 10.1029/JB095iB08p12653.
[94] J. Kirby, D. Saunders, Fading and colour change of Prussian blue: methods of manufacture and the influence of extenders, National Gallery Technical Bulletin 25 (2004) 73–99.
[95] C. Korenberg, The photo-ageing behaviour of selected watercolour paints under anoxic conditions, National Gallery Technical Bulletin 2 (2008) 49-57.

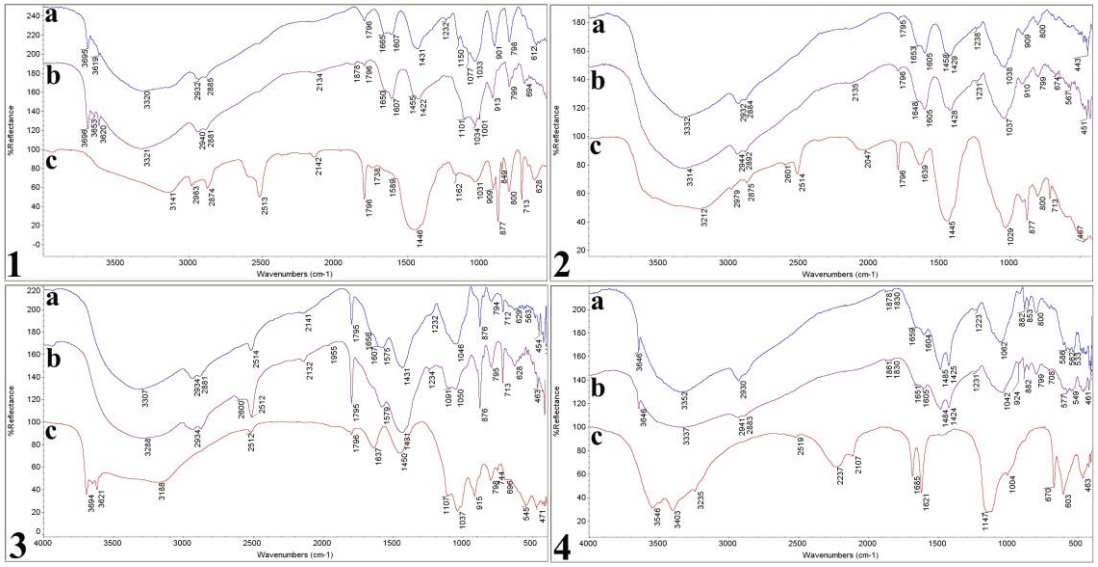

Fig. 1 FT-IR spectra of the selected pigments and watercolours before application. 1) yellow ochre; 2) raw umber; 3) raw Sienna; and 4) Venetian red. a) spectrum of pan sample, b) spectrum of tube sample and c) spectrum of powder sample.

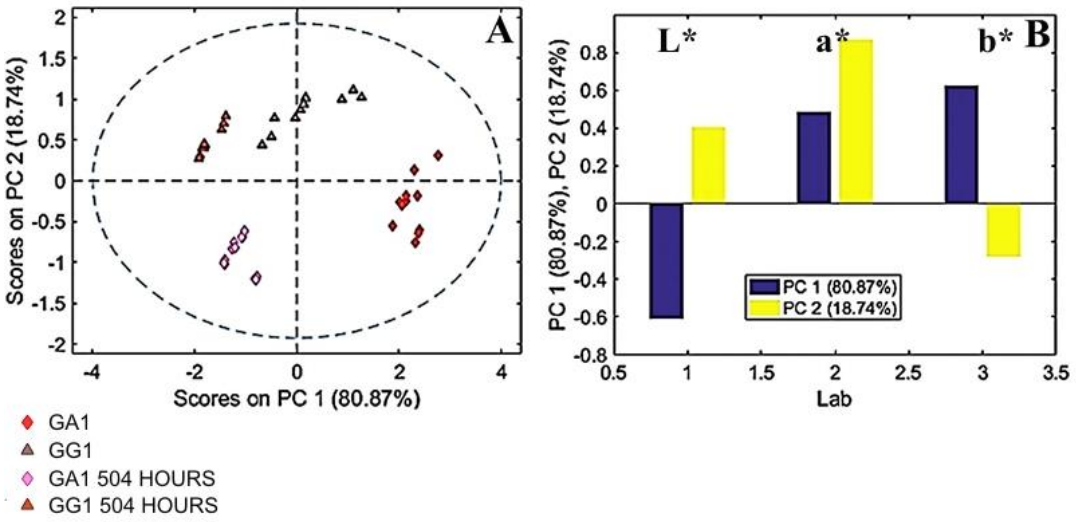

Fig. 2 PCA score plot (A) and loadings (B) related to CIELAB1976 colour system chromatic coordinates for gum Arabic (GA) and ground layer (GG) at 0 and 504 hours of irradiation.

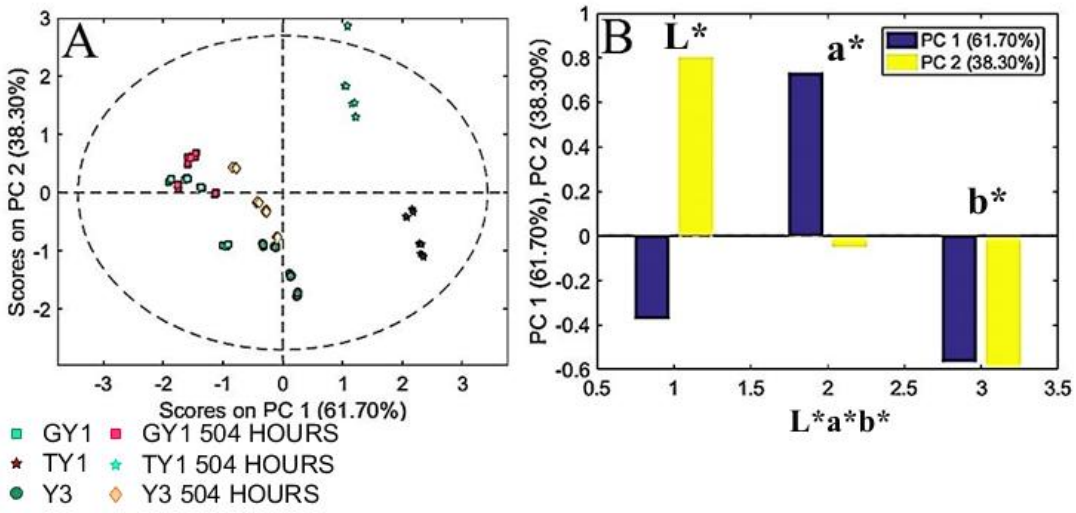

Fig. 3 PCA score plot (A) and loadings (B) related to CIELAB1976 colour system chromatic coordinates for yellow ochre painting samples at 0 and 504 hours of irradiation.

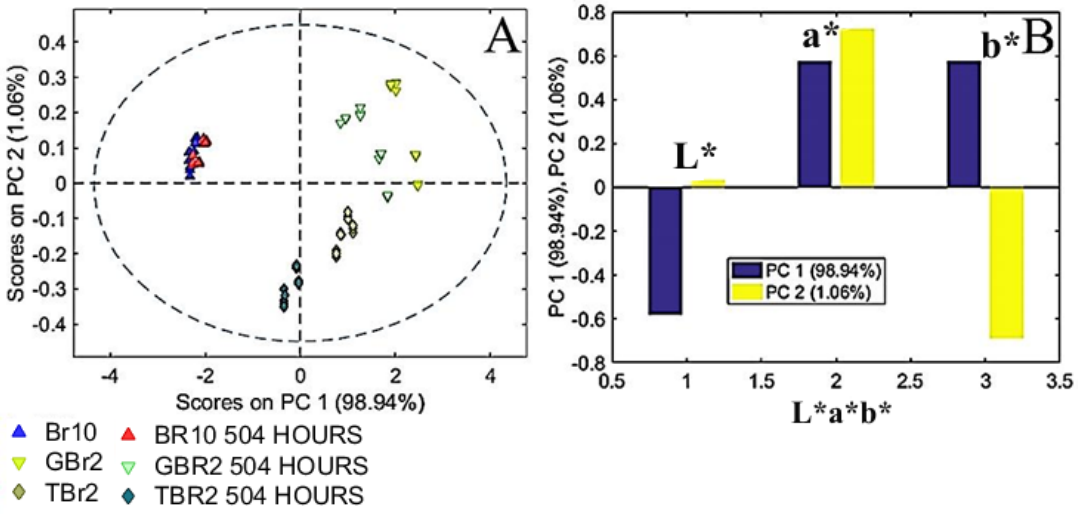

Fig. 4 PCA score plot (A) and loadings (B) related to CIELAB1976 colour system chromatic coordinates for raw umber painting samples at 0 and 504 hours of irradiation.

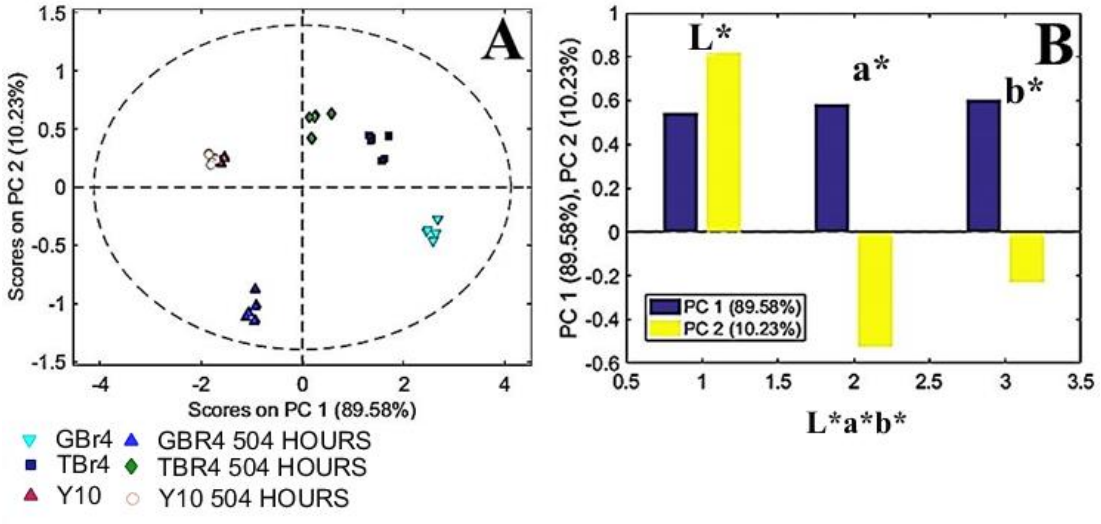

Fig. 5 PCA score plot (A) and loadings (B) related to CIELAB1976 colour system chromatic coordinates for raw Sienna samples at 0 and 504 hours of irradiation.

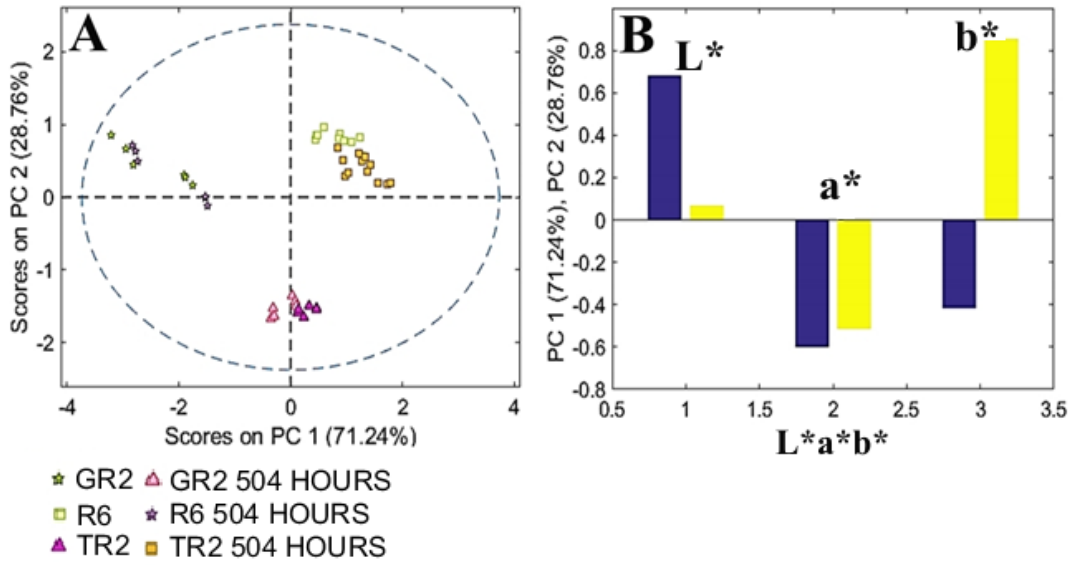

Fig. 6 PCA score plot (A) and loadings (B) related to CIELAB1976 colour system chromatic coordinates for Venetian red painting samples at 0 and 504 hours of irradiation.

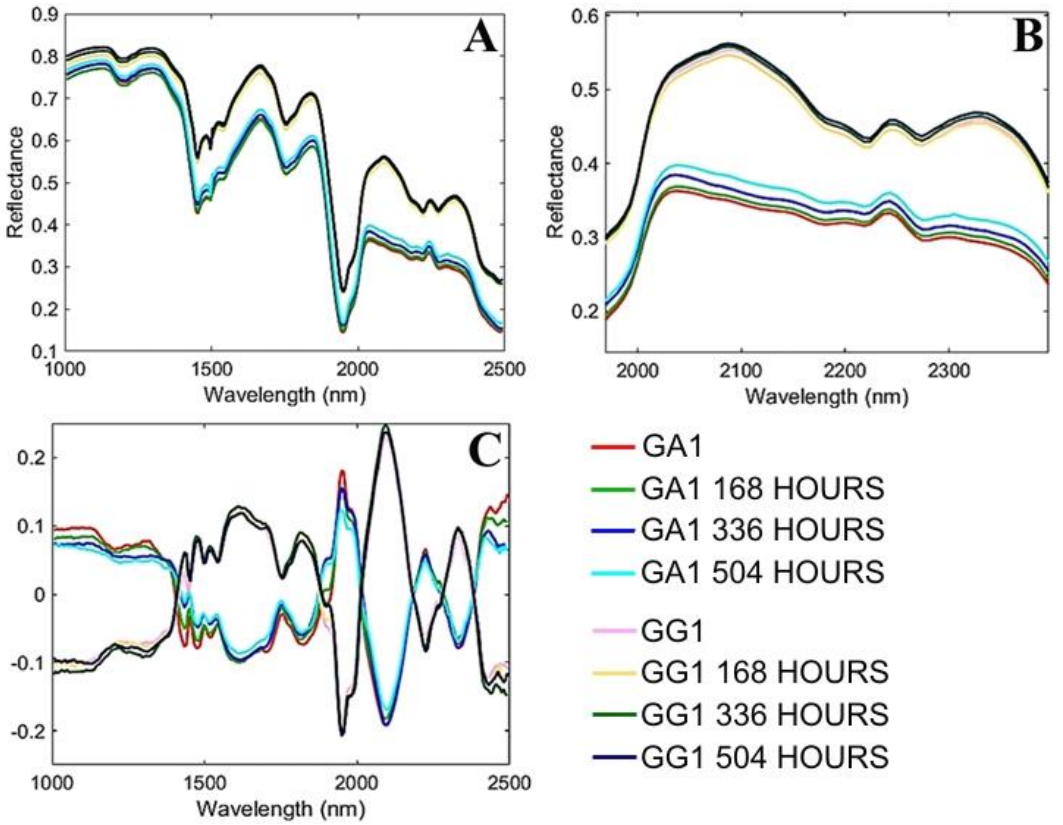

Fig. 7 Average spectra (A), detail of spectra in the range 2000-2400 nm (B) and pre-processed spectra (C), for gum Arabic (GA1) and ground layer (GG1).

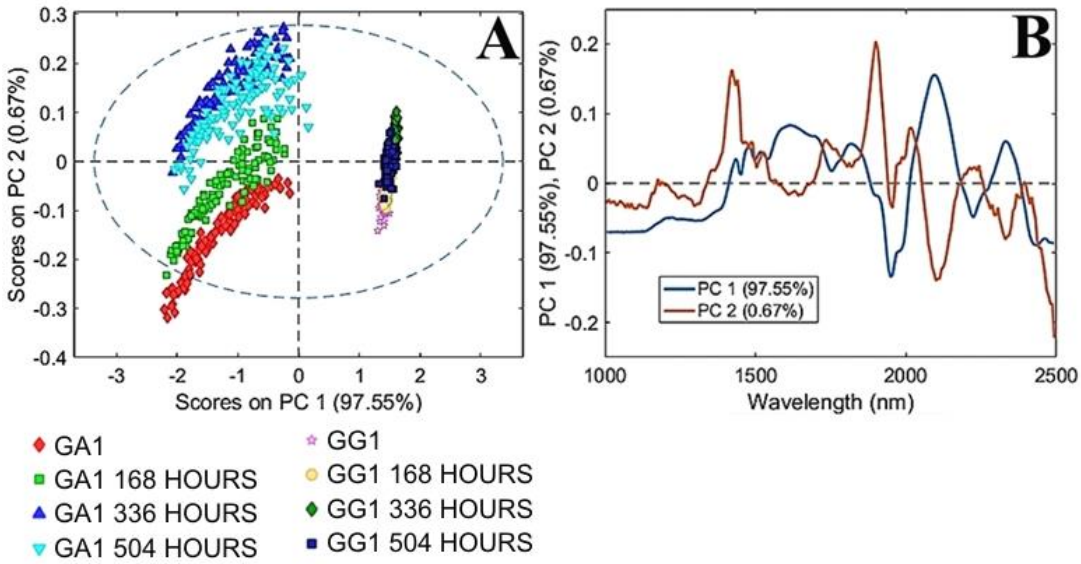

Fig. 8 PCA score plot (A) and loadings (B) for gum Arabic and ground layer at the different ageing times.

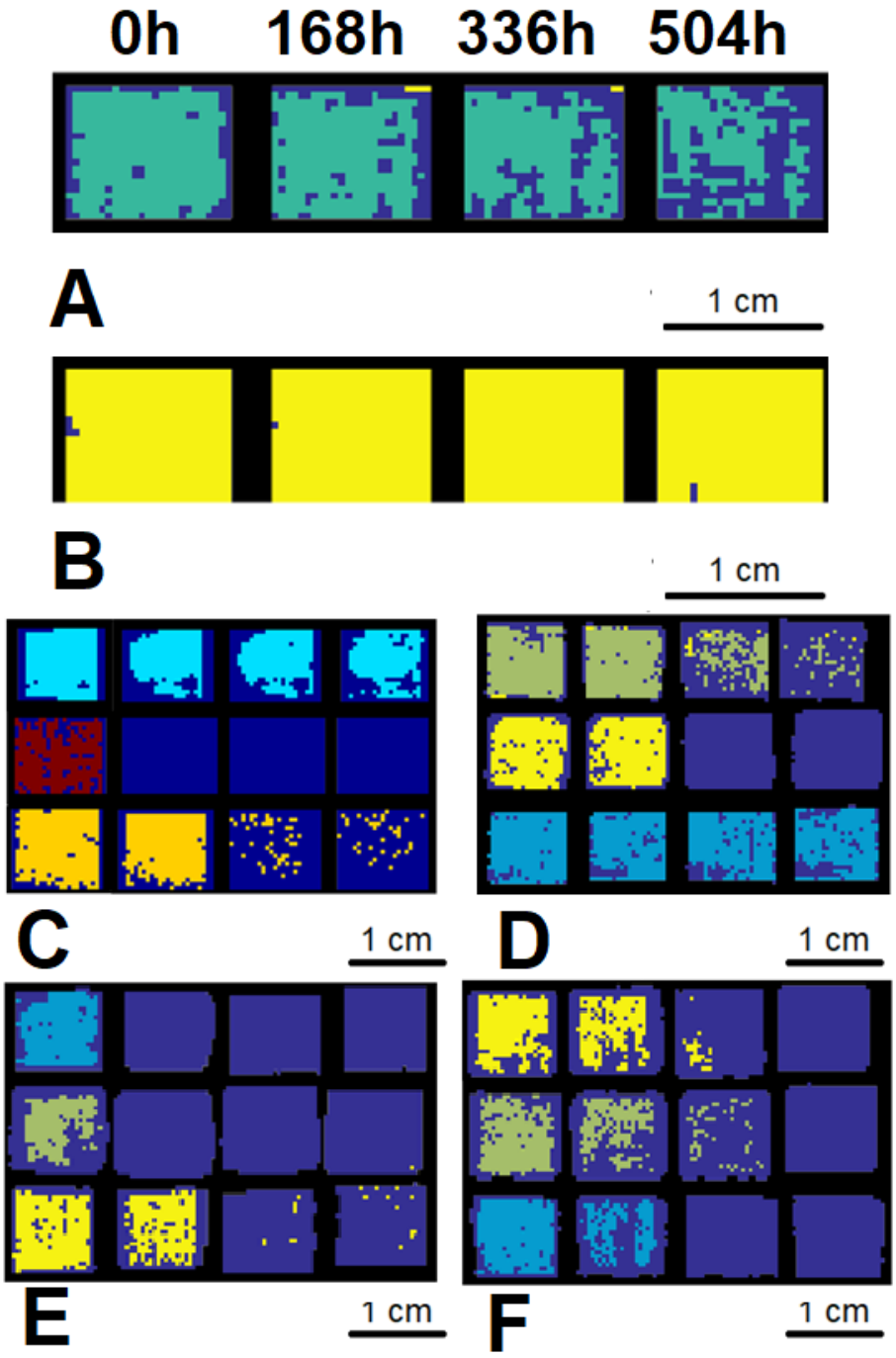

Fig. 9 Results of Soft Independent Modelling of Class Analogy Classification (SIMCA) model applied to painting samples. The model shows the variation (from left to right) of the surfaces with irradiation time. A) Gum Arabic; B) ground layer; C) yellow ochre painting samples; D) raw umber painting samples; E) raw Sienna painting samples; F) Venetian red painting samples. In C-F: upper row is the pan watercolour, central row is tube and lower one is powder pigment

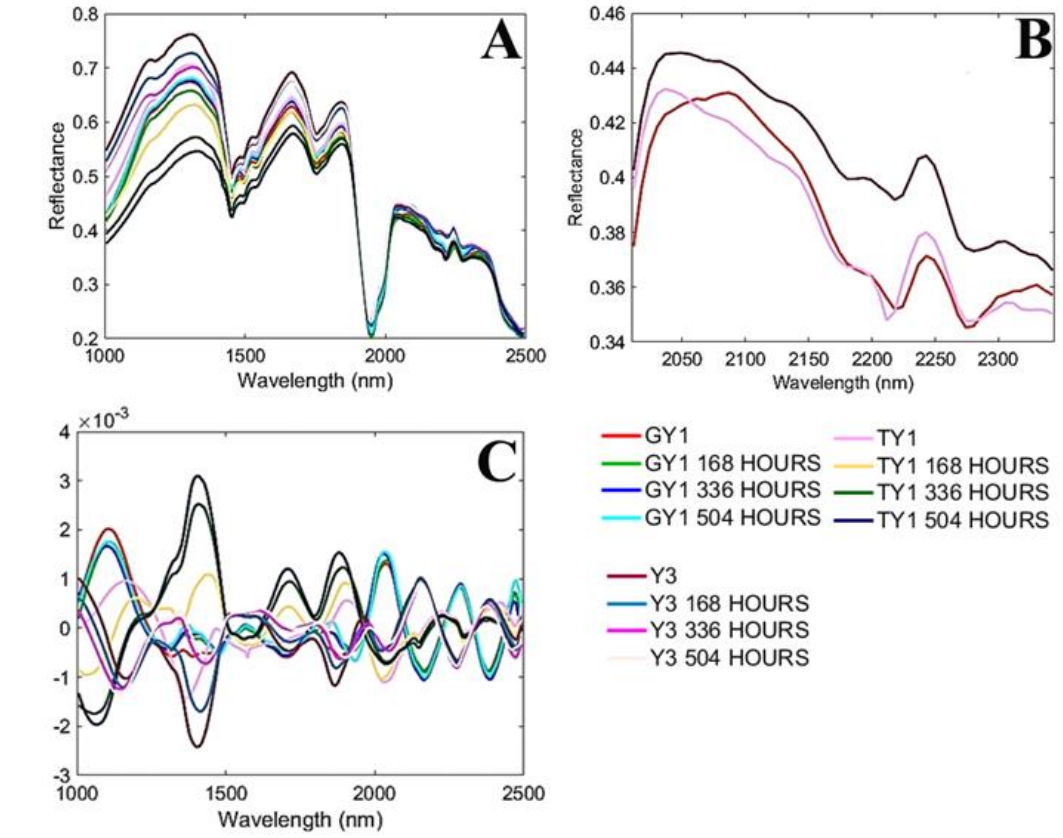

Fig. 10 Average spectra (A), detail of spectra in the range 2000-2350 nm (B) and pre-processed spectra (C), for yellow ochre painting samples.

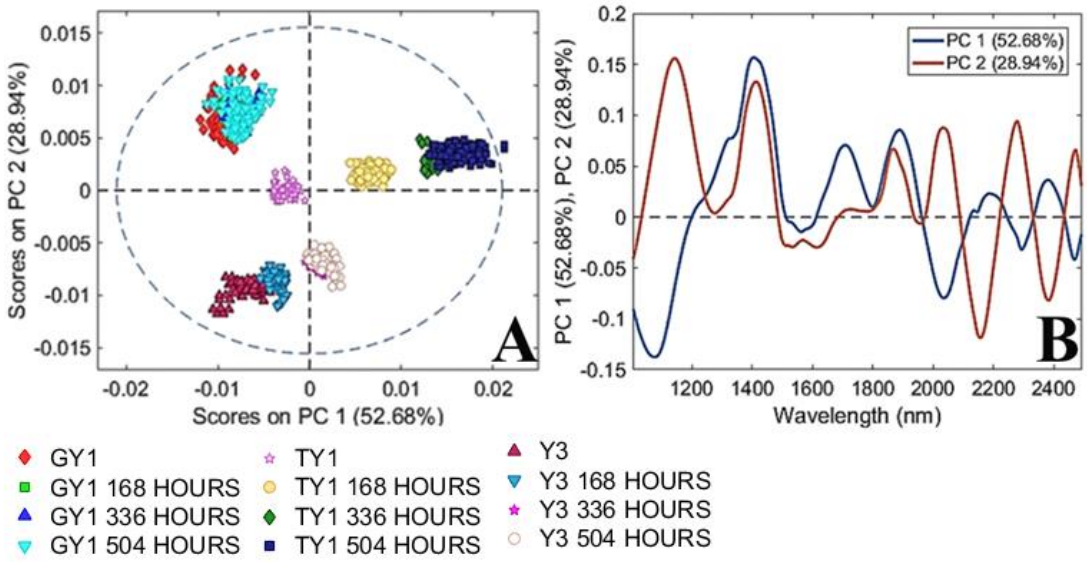

Fig. 11 PCA score plot (A) and loadings (B) for yellow ochre painting samples at the different ageing times.

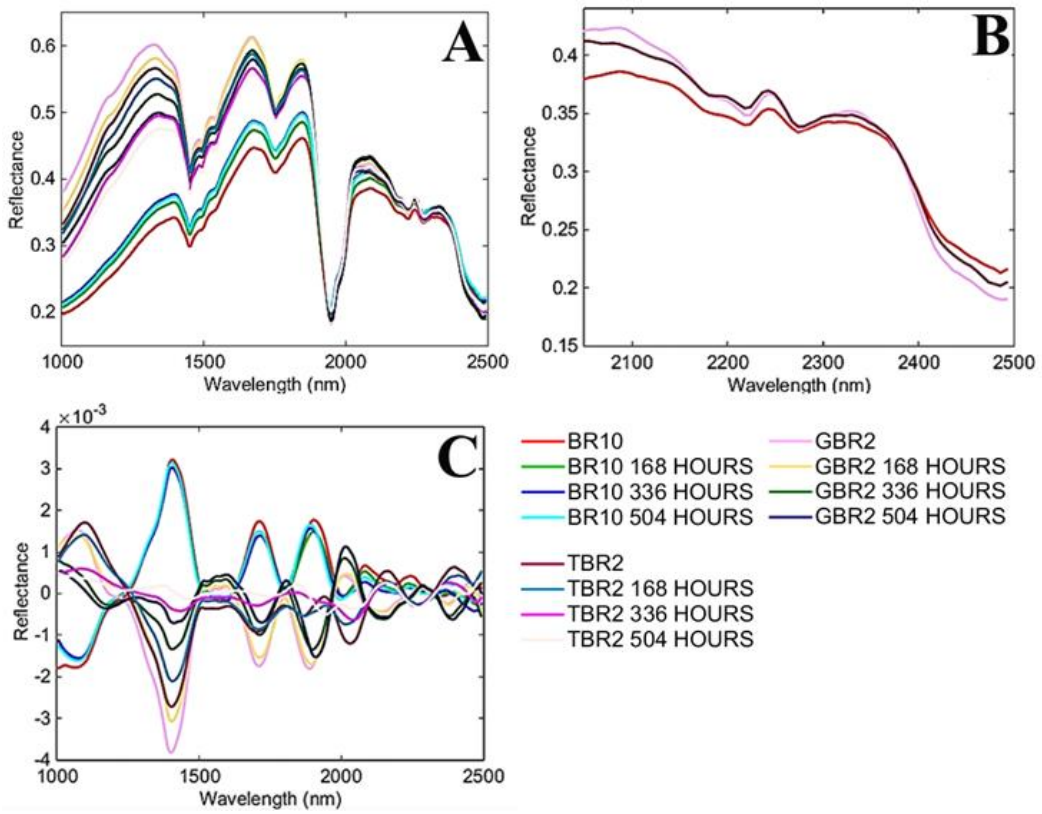

Fig. 12 Average spectra (A), detail of spectra in the range 2050-2500 nm (B) and pre-processed spectra (C), for raw umber painting samples.

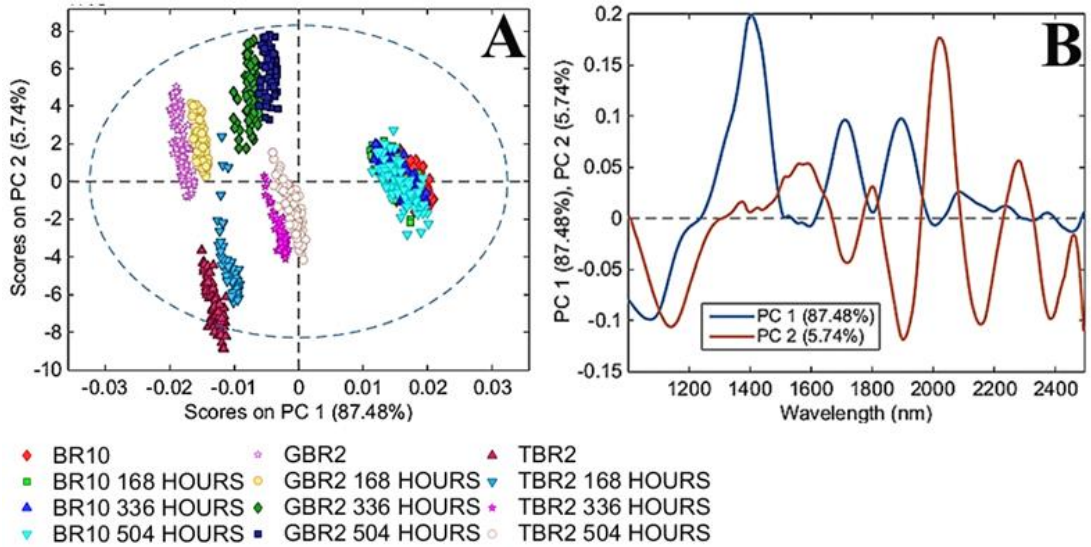

Fig. 13 PCA score plot (A) and loadings (B) for raw umber painting samples at the different ageing times.

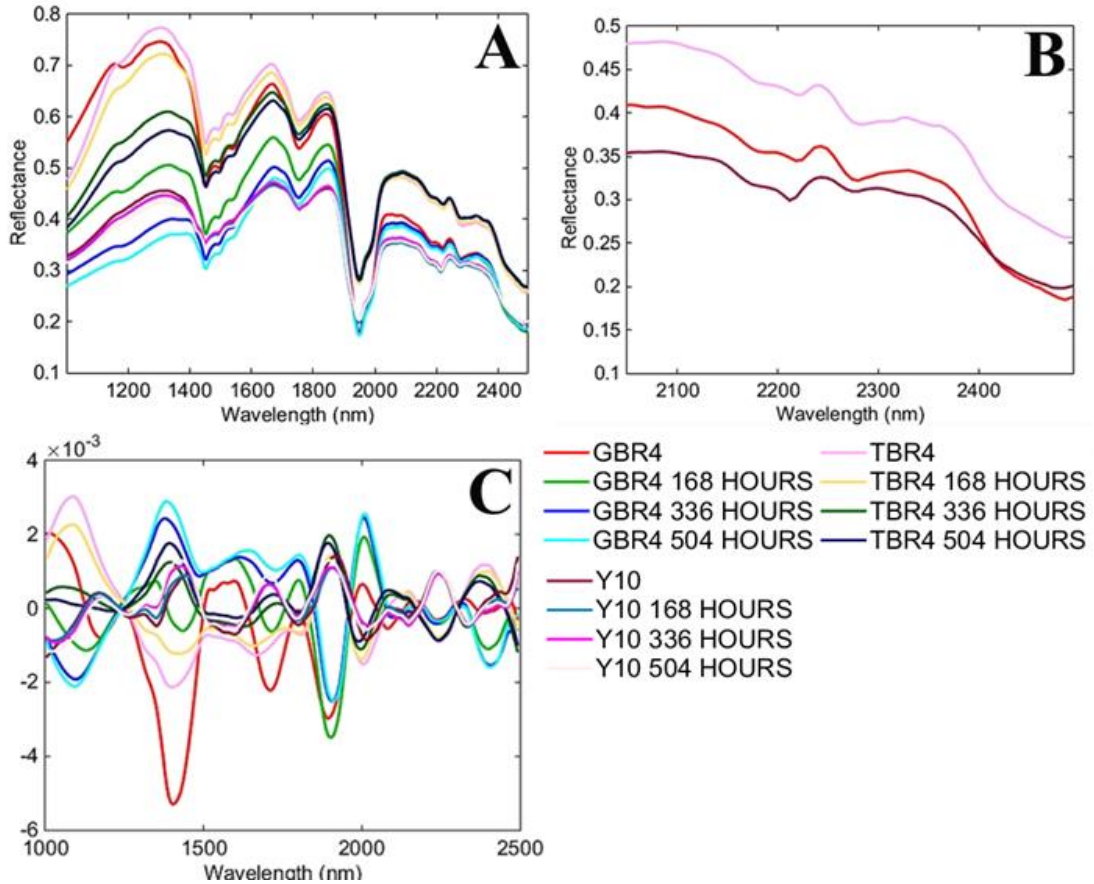

Fig. 14 Average spectra (A), detail of spectra in the range 2050-2500 nm (B) and pre-processed spectra (C), for raw Sienna painting samples.

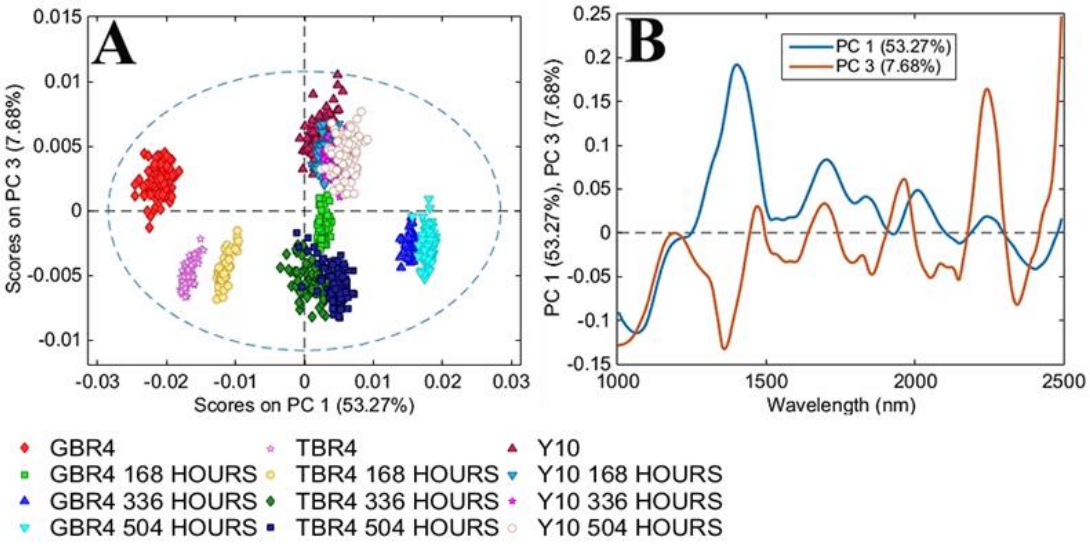

Fig. 15 PCA score plot (A) and loadings (B) for raw Sienna painting samples at the different ageing times.

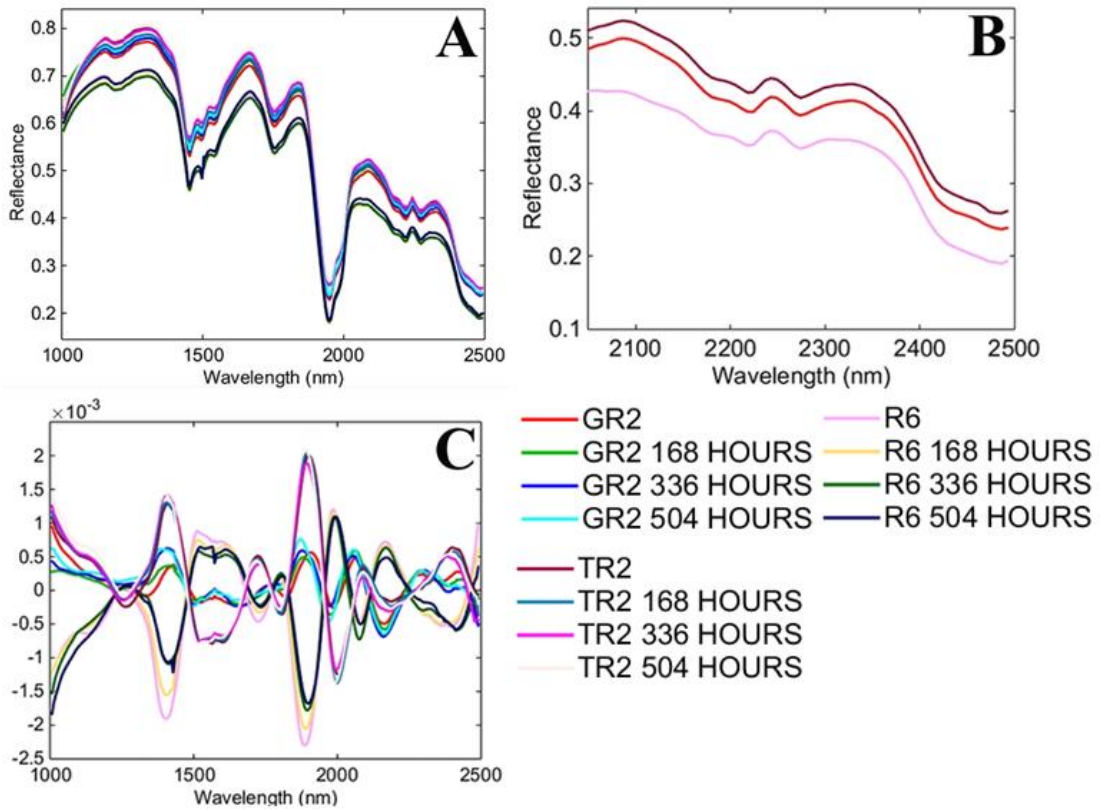

Fig. 16 Average spectra (A), detail of spectra in the range 2050-2500 nm (B) and pre-processed spectra (C), for Venetian red painting samples.

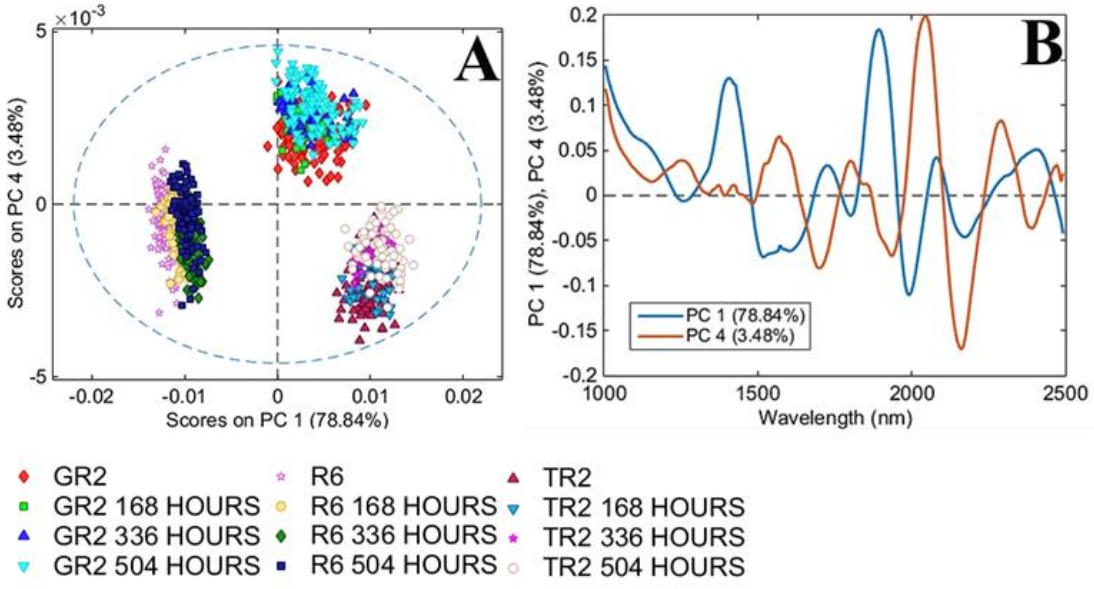

Fig. 17 PCA score plot (A) and loadings (B) for Venetian red painting samples at the different ageing times.

Table 1 – List of chosen samples with description

Sample abbreviations	Description
GG	Ground layer made of gypsum and glue
GA	Gum Arabic applied on ground layer by brush
GY1	Yellow ochre by W&N in pan format
TY1	Yellow ochre by W&N in tube format
Y3	Yellow ochre in powder from Provence (France)
GBR2	Raw umber by W&N in pan format
TBR2	Raw umber by W&N in tune format
BR10	Raw umber in powder from Sicily (Italy)
GBR4	Raw Sienna by W&N in pan format
TBR4	Raw Sienna by W&N in tube format
Y10	Raw Sienna in powder from Tuscany (Italy)
GR2	Venetian red by W&N in pan format
TR2	Venetian red in tube format
R6	Venetian red in powder from Veneto (Italy)

Table 2 – Chromatic coordinate differences at each ageing time.

Sample	ΔL*	Δa*	Δb*	ΔE*
GA	1.98 (168h)	-0.30 (168h)	-3.15 (168h)	3.74 (168h)
	2.58 (336h)	-0.40 (336h)	-4.45 (336h)	5.16 (336h)
	2.63 (504h)	-0.47 (504h)	-4.80 (504h)	5.50 (504h)
GG	1.47 (168h)	-0.25 (168h)	-2.01 (168h)	2.57 (168h)
	1.48 (336h)	-0.30 (336h)	-2.71 (336h)	3.10 (336h)
	1.56 (504h)	-0.33 (504h)	-2.54 (504h)	3.00 (504h)
GY1	-0.13 (168h)	-0.11 (168h)	-0.31 (168h)	0.46 (168h)
	-0.22 (336h)	-0.22 (336h)	-0.79 (336h)	0.85 (336h)
	-0.44 (504h)	-0.34 (504h)	-0.99 (504h)	1.14 (504h)
TY1	-1.18 (168h)	-1.24 (168h)	-1.35 (168h)	2.18 (168h)
	-1.96 (336h)	-3.01 (336h)	-4.30 (336h)	5.60 (336h)
	-2.21 (504h)	-3.41 (504h)	-4.79 (504h)	6.29 (504h)
Y3	-0.80 (168h)	-0.81 (168h)	-1.55 (168h)	1.92 (168h)
	-1.58 (336h)	-1.57 (336h)	-2.87 (336h)	3.63 (336h)
	-1.61 (504h)	-1.60 (504h)	-2.85(504h)	3.64 (504h)
GBR2	-2.23 (168h)	-2.47 (168h)	-2.73 (168h)	4.31 (168h)
	-3.08 (336h)	-4.13 (336h)	-4.96 (336h)	7.15 (336h)
	-3.23 (504h)	-4.47 (504h)	-5.49 (504)	7.78 (504h)
TBR2	-1.49 (168h)	-2.16 (168h)	-2.41 (168h)	3.56 (168h)
	-2.01 (336h)	-3.40 (336h)	-4.02 (336h)	5.63 (336h)
	-2.20 (504h)	-3.71 (504h)	-4.36 (504h)	6.13 (504h)
BR10	0.71 (168h)	0.12 (168h)	0.27 (168h)	0.77 (168h)
	0.72 (336h)	0.24 (336h)	0.39 (336h)	0.85 (336h)
	0.71 (504h)	0.27 (504h)	0.41 (504h)	0.87 (504h)
GBR4	-6.40 (168h)	-5.80 (168h)	-10.3 (168h)	13.4 (168h)
	-9.62 (336h)	-8.92 (336h)	-15.5 (336h)	20.3 (336h)
	-10.3 (504h)	-9.61 (504h)	-16.7 (504h)	21.9 (504h)
TBR4	-1.11 (168h)	-2.34 (168h)	-3.59 (168h)	4.43 (168h)
	-2.20 (336h)	-4.25 (336h)	-6.38 (336h)	7.97 (336h)
	-2.08 (504h)	-4.41 (504h)	-6.57 (504h)	8.18 (504h)
Y10	-0.21 (168h)	-0.34 (168h)	-0.33 (168h)	0.52 (168h)
	-0.56 (336h)	-0.64 (336h)	-0.82 (336h)	1.18 (336h)
	-0.41 (504h)	-0.71 (504h)	-0.95 (504h)	1.26 (504h)
GR2	-0.02 (168h)	-0.05 (168h)	-0.07 (168h)	0.09 (168h)
	-0.09 (336h)	-0.18 (336h)	-0.12 (336h)	0.23 (336h)
	-0.20 (504h)	-0.17 (504h)	-0.17 (504h)	0.31 (504h)
TR2	-0.15 (168h)	-0.15 (168h)	-0.17 (168h)	0.27 (168h)
	-0.82 (336h)	-0.54 (336h)	-0.43 (336h)	1.07 (336h)
	-0.37 (504h)	-0.37 (504h)	-0.43 (504h)	0.68 (504h)
R6	0.11 (168h)	-0.16 (168h)	-0.10 (168h)	0.22 (168h)
	0.21 (336h)	-0.20 (336h)	-0.19 (336h)	0.35 (336h)
	0.22 (504h)	-0.06 (504h)	-0.03 (504h)	0.23 (504h)